PLOS ONE

RESEARCH ARTICLE

Medial septal cholinergic mediation of hippocampal theta rhythm induced by vagal nerve stimulation

Adam Broncel[1], **Renata Bocian**[2], **Paulina Kłos-Wojtczak**[1,2], **Jan Konopacki**[2]*

1 Neuromedical, Research Department, Łódź, Poland, **2** Department of Neurobiology, Faculty of Biology and Environmental Protection, The University of Łódź, Łódź, Poland

* jan.konopacki@biol.uni.lodz.pl

OPEN ACCESS

Citation: Broncel A, Bocian R, Kłos-Wojtczak P, Konopacki J (2018) Medial septal cholinergic mediation of hippocampal theta rhythm induced by vagal nerve stimulation. PLoS ONE 13(11): e0206532. https://doi.org/10.1371/journal.pone.0206532

Editor: Giuseppe Biagini, University of Modena and Reggio Emilia, ITALY

Received: March 14, 2018

Accepted: October 15, 2018

Published: November 5, 2018

Data Availability Statement: All relevant data are within the paper.

Funding: This work was supported by grant from Regional Operational Programme for Lodzkie Voivodeship for 2014–2020 (grant number: RPLD.01.02.02-10-0067/17-00).

Competing interests: The authors have declared that no competing interests exist.

Abstract

Background

Electrical vagal nerve stimulation (VNS) has been used for years to treat patients with drug-resistant epilepsy. This technique also remains under investigation as a specific treatment of patients with Alzheimer's disease. Recently we discovered that VNS induced hippocampal formation (HPC) type II theta rhythm, which is involved in memory consolidation. In the present study, we have extended our previous observation and addressed the neuronal substrate and pharmacological profile of HPC type II theta rhythm induced by VNS in anesthetized rats.

Methods

Male Wistar rats were implanted with a VNS cuff electrode around the left vagus nerve, a tungsten microelectrode for recording the HPC field activity, and a medial septal (MS) cannula for the injection of a local anesthetic, procaine, and muscarinic agents. A direct, brief effect of VNS on the HPC field potential was evaluated before and after medial-septal drug injection.

Results

Medial septal injection of local anesthetic, procaine, reversibly abolished VNS-induced HPC theta rhythm. With the use of cholinergic muscarinic agonist and antagonists, we demonstrated that medial septal M1 receptors are involved in the mediation of the VNS effect on HPC theta field potential.

Conclusion

The MS cholinergic M1 receptor mechanism integrates not only central inputs from the brainstem synchronizing pathway, which underlies the production of HPC type II theta rhythm, but also the input from the vagal afferents in the brain stem.

Introduction

Electrical vagal nerve stimulation (VNS) has been used for years to treat patients with drug-resistant epilepsy [1–5]. Although VNS was approved as adjunctive therapy for reducing the frequency of seizures in adults and adolescents, the mechanisms through which VNS modulates activity in the central nervous system are still poorly understood. Interestingly, this technique also remains under investigation as a specific treatment for several other psychiatric and neurological disorders. Among these, VNS is used for the treatment of Alzheimer's disease [6], depression [4,7,8], schizophrenia [9], migraine [10,11] and central inflammation [12,13]. In addition, VNS has been found to enhance motor and cognitive function in animal models of traumatic brain injury [14], increase alertness [15], enhance the extinction of conditioned fear [16] and alter norepinephrine, dopamine, serotonin and GABA levels in the hippocampal formation (HPC) [17,18]. Interestingly, VNS has also been demonstrated to enhance HPC-induced long-term potentiation (LTP) [19,20] and improve memory in rats and humans [21–23]. The latter findings suggest that VNS may affect memory by enhancing neural plasticity in brain structures associated with memory storage, such as the HPC. This memory processing is related to an increase in the excitation of the hippocampal neuronal network and the presence of a local theta rhythm [24–29]. In agreement with this suggestion, Broncel et al. [30], using several experimental protocols, have recently demonstrated that VNS induced the HPC theta rhythm in anesthetized rats. This was the first direct finding demonstrating the vagal nerve to be involved in central mechanisms underlying oscillations and synchrony in limbic cortex.

The fundamental question arises as to the neuronal substrate and pharmacological profile underlying the effect of VNS on HPC theta. The vagal nerve is a major component of the parasympathetic nervous system and plays a key role in the neuroendocrine-immune axis to maintain homeostasis. It is a mixed cranial nerve consisting of 20% efferent and 80% afferent fibres. The nucleus of the solitary tract (NST), being the main vagal relay site in the brain, receives the most vagal afferents [31]. This nucleus in turn projects to several structures including the locus coeruleus, periaqueductal grey matter, dorsal raphe nucleus, paraventricular thalamic nucleus, amygdala and the medial septum [32–36]. However, there is no direct anatomical projection from the NST to the hippocampal formation [37]. These findings suggest that vagal input might be passed through the NST, and then reaches the HPC probably through the next multisynaptic pathway that has not been yet described. It seems that the medial septal nucleus and the vertical limb of the nucleus of the diagonal band of Broca (MS/vDBB) is the best candidate for carrying the vagal input from the NST to the hippocampal formation. This region functions as the node in ascending pathways, sending inputs to the HPC [38,39]. It is widely known that MS/vDBB cells act as a pacemaker for discharges of hippocampal neurons responsible for theta production [38,40–42]. In addition, this region is the principal source of strong cholinergic innervation of HPC [38,43–48] which was previously demonstrated to determine the production of HPC type II theta rhythm [38,44,49,50].

The purpose of the present study was to test the hypotheses that: i/ the medial septal region mediates the effect of VNS on HPC type II theta, and ii/ this mediation has a cholinergic profile. Portions of these data have appeared in abstract form [51,52].

Materials and methods

The studies described below were approved and monitored by Local Ethics Committee for Animal Experiments in Lodz (Permissions Number: 5/LB13/2016). All surgery was performed under anesthesia, and all efforts were made to minimize suffering.

Subjects and surgical procedure

The data were obtained from 35 male Wistar rats (120–150 g) housed on a 12 h light/dark cycle with free access to water and food. The rats were initially anesthetized with isoflurane (Baxter, Belgium) while a jugular cannula was inserted. Isoflurane was then discontinued, and urethane (0.6 g/ml, Sigma Chemical Co., USA) was administered via the jugular cannula in order to maintain anesthesia throughout the experiment. Anesthesia levels were maintained such that theta field potentials and the transition from theta to large irregular activity (LIA) could occur spontaneously. Body temperature was maintained at 36.5 ± 0.5˚C by a heating pad, and heart rate was monitored constantly throughout the experiment.

Vagal electrode implantation

Since it is generally observed that left VNS minimizes potential cardiac effects, such as bradycardia or asystole [4], in the second stage of the procedure, the left cervical-vagal nerve was gently separated from the muscles and then isolated from the carotid artery using glass section sticks. Before implantation of the stimulating electrode, the vagal nerve was moisturized with glycerine. A custom-made platinum-iridium cuff electrode (SPM35 10HY, MicroProbe, USA) was gently placed around the vagal nerve (Fig 1A). The platinum-iridium wire leads were tunnelled subcutaneously for about 2 cm and then connected with the input from a PSIU6 isolation unit (Grass-Astromed, West Warwick, USA).

Hippocampal electrode implantation

The rats were placed in a stereotaxic frame with the plane between bregma and lambda levelled to horizontal. An uninsulated tungsten wire placed in the cortex, 2 mm anterior to bregma, served as an indifferent electrode, and the stereotaxic frame was connected to the ground. A tungsten microelectrode (0.1–0.9 MΩ) for recording the hippocampal field activity was placed in the right dorsal HPC, in the stratum lacunosum-moleculare (3.7 mm posterior to bregma, 2.0–2.2 mm lateral from the midline and 2.6–2.9 mm ventral to the dural surface [53]; Fig 1B). An AC amplifier (P-511, Grass-Astromed, West Warwick, USA) was used for recording field

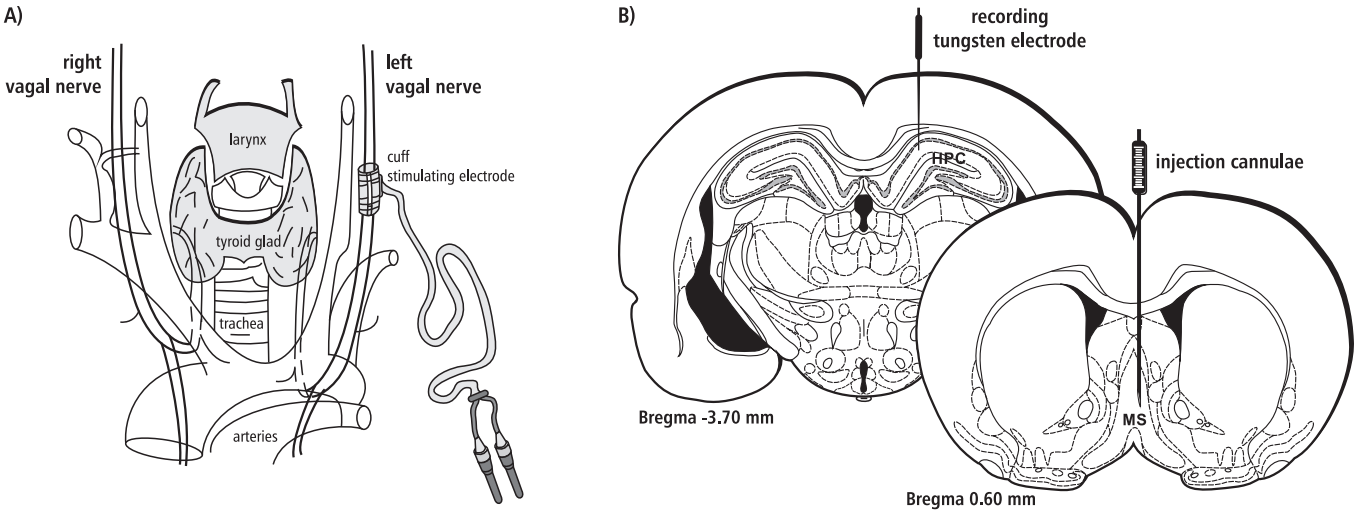

Fig 1. A diagrammatic representation of the electrode implantation arrangement. (A) The platinum-iridium cuff stimulating electrode was positioned on the left vagal nerve. (B) The recording electrode was implanted in the right hippocampal formation and the injection cannula in the right medial septum (see details in the text).

https://doi.org/10.1371/journal.pone.0206532.g001

potentials, with the low filter set at 1 Hz and the high filter set at 0.3 kHz. The mentioned band pass filter was applied to the data prior to any analysis. The field activity was displayed using a digital storage oscilloscope (Tektronix TDS 3014, USA) and a PC computer (Spike 2.7, Cambridge Electronic Design, GB). EEG signals were digitalized by interface (1410 plus, Cambridge Electronic Design, GB) and recorded onto a computer hard disk for subsequent off-line analysis. After the optimal HPC field potential was obtained (theta amplitude of at least 400 μV), the electrode was fixed to the skull with dental cement.

Medial septal cannula implantation and injections

In preliminary experiments, we did not find evidence for the lateralization of the effects of intraseptal injection of drugs used on hippocampal theta (data not shown). Hence, in the initial experiments, microinjection (26 gauge, 5 ml Hamilton 701N microsyringe) of saline and all agents used were always performed into the right MS (Fig 1B). The coordinates of Hamilton canulae were as follows: 0.6 mm superior from bregma, 0.3 mm lateral from the midline, and 6.5–7.0 mm ventral to the dural surface [53]. All 35 animals receiving the drug injection to the medial septum were divided into six experimental groups (5 or 6 animals each, Table 1): 1/ The animals of group I were administrated with 1 μl of 0.9% NaCl. 2/ The animals of group II were administrated with a local anesthetic, 1 μl procaine hydrochloride (20%). 3/ The animals of group III were injected with cholinergic receptor antagonist atropine sulphate (20 μg/1μl). 4/ The animals of group IV were administrated with cholinergic M1 receptor antagonist dicyclomine hydrochloride (4μg/1 μl). 5/ The animals of group V were administrated with cholinergic M2 receptor antagonist gallamine triethiodide (2 μl/1 μl). 6/ The animals of group VI were injected with selective M1 receptor agonist McN-A343 (0.5 μl/1μl). All drugs used in this study were obtained from the Sigma Chemical Corporation (St. Louis, USA) and injected into the region of the medial septum at the same rate of 1 μl/30 s. The threshold concentration of procaine hydrochloride and atropine sulphate were developed previously [54, 55] and the threshold concentrations of dicyclomine hydrochloride, gallamine triethiodide and McN-A343 were developed in preliminary experiments (data not shown).

Vagal nerve stimulation

Based on our previous experiments [30], in the present study, the following square pulse parameters were applied: pulse duration (1 ms), train duration (10 s), frequency (10 Hz) and current intensity of 8 mA. These VNS parameters were previously found to induce a direct, brief effect on HPC field potential, i.e., theta rhythm appearing during vagal stimulation. VNS was delivered through a PSIU6 isolation unit (Grass-Astromed, West Warwick, USA) from an S48 square pulse stimulator (Grass-Astromed, West Warwick, USA). VNS was applied twice or three times, depending on the applied protocol (Fig 2). In each protocol, the medial-septal drug injection was pre-treated by 5 min HPC field recording while 10 s VNS was applied

Table 1. Experimental group and injection compounds.

Group	Place of injection	Compound	Dose/volume	Number of animals
Group I	medial septum	NaCl	0.9%/1μl	5
Group II		procaine hydrochloride	20%/1μl	6
Group III		atropine sulphate	20 μg/1μl	6
Group IV		dicyclomine hydrochloride	4 μg/1μl	6
Group V		gallamine triethiodide	2 μg/1μl	6
Group VI		McN-A343	0.5 μg/1μl	6

https://doi.org/10.1371/journal.pone.0206532.t001

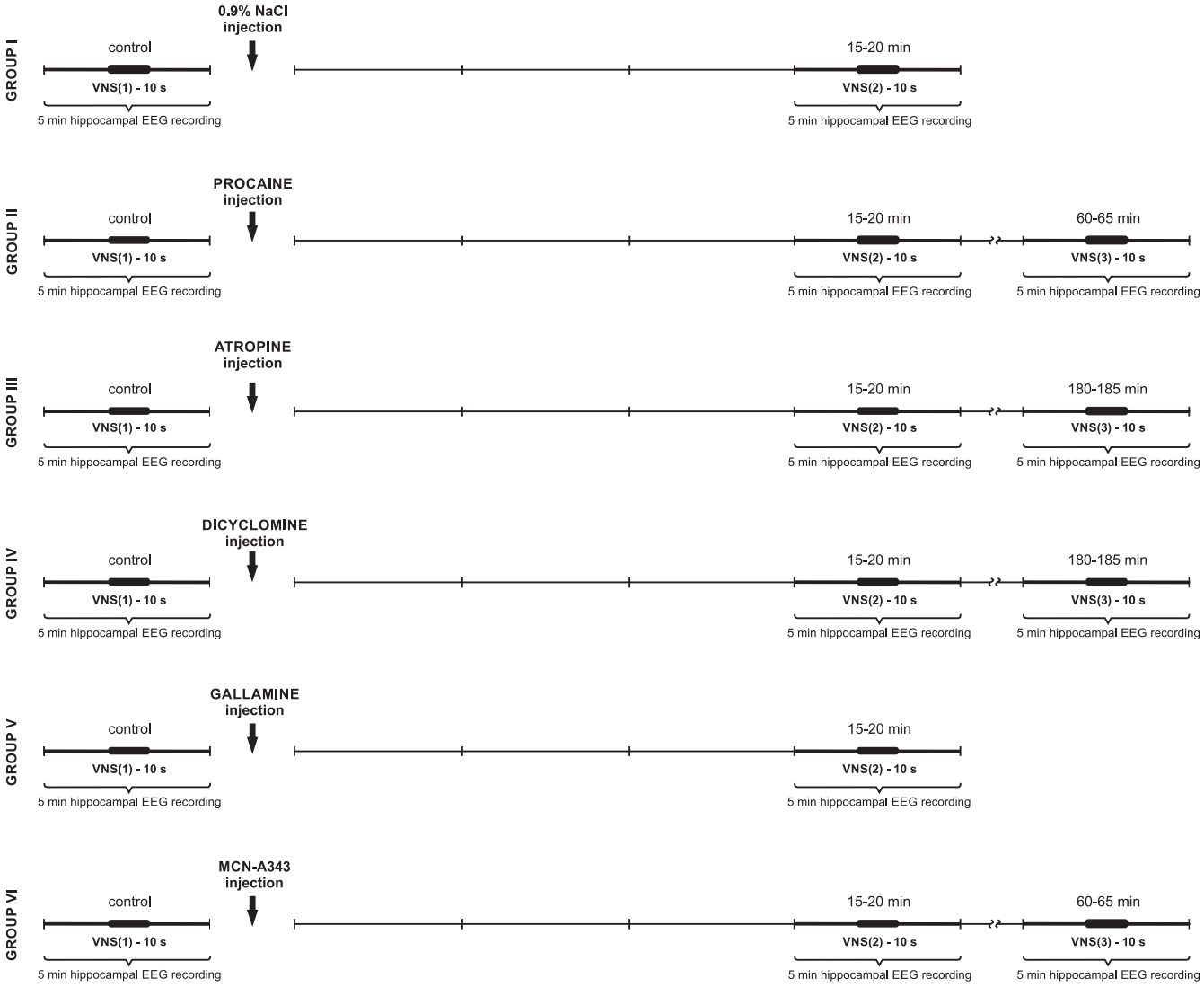

Fig 2. A schematic arrangement of protocols applied in each experimental group (I-VI). Each 5-min pre- and post-VNS period is marked with a thin vertical line. Each 10-s VNS is marked with a thick line (see details in the text).

https://doi.org/10.1371/journal.pone.0206532.g002

(control). The VNS was always applied at a moment when no spontaneous theta was present in the HPC field potentials.

Experimental protocols

Initially, the experiments were performed on 39 rats, but only 35 animals were taken into consideration (in four animals, the injection sites in the medial septum were incorrect). Thirty five rats were divided into six experimental groups in which different arrangements of VNS and HPC field potential recording were applied (Fig 2). As shown in Fig 2, in groups I and V, VNS was applied twice: in control, pre-injection time and after the injection, between the 15 and 20 min. In groups II, III, IV and VI, VNS was applied three times: in control, pre-injection time and twice post-injection: between the 15–20 min and then between the 60 and 65 min (group II and VI) or 180 and 185 min (groups III and IV).

Recording procedure and data analysis

HPC field activity was recorded continuously and analyzed in five-minute panels before drug injection and at strictly defined times after the medial-septal drug injection, (see Fig 2). Power spectra in the 0–50 Hz range for the 10 s HPC field potential recordings obtained during each VNS session were generated using the fast Fourier transform (FFT) algorithm implemented in the Spike 2.7 software package (Cambridge Electronic Design, GB) after a Hanning window was applied to the time series, which were obtained at a sample rate of 100 Hz.

In this study, theta epochs were defined as rhythmic high amplitude sinusoidal waveforms in a strictly defined frequency band (3–6 Hz). These were identified by peaks in the power spectra within that frequency band, and confirmed by visual inspection of the raw EEG traces. Theta frequency for each 10s VNS epoch was then defined as the frequency with maximum power within the 3–6 Hz range, and theta power for each 10s VNS epoch as the peak power value within the same frequency range.

Statistics

Mean values and standard errors of the mean (± SEM) of two measured theta parameters (power and frequency) obtained during VNS performed before the medial septal drug injection and in successive time periods after the injection were computed and compared. The power and frequency of HPC theta rhythm induced during VNS, before and after the medial-septal drug injections, were subjected to the Shapiro-Wilk test to check the normal distribution of the data. Then, the Mann-Whitney U test was performed (StatSoft Poland).

Histological procedure

The recording electrode tip location was marked by passing 15 μA current for 14 min (7 min cathodal, 7 min anodal, S48 stimulator; Grass-Astromed, West Warwick, USA). Next, the rat was sacrificed by an overdose of urethane for histological examination. The brain was removed and stored in 10% formalin. Frozen brain sections (30 μm) were taken serially and mounted on glass slides for the reconstruction of the medial septal injection sites and the evaluation of HPC theta recording sites (data not shown).

Results

Only data obtained in experiments performed on rats with the correct location of the HPC recording sites and the correct medial septal injection sites were presented in this study (n = 35). Fig 3 provides microphotographs and a diagrammatic reconstruction [53] of representative locations of the injection sites in the medial septum in three representative rat preparations of each group (18 sites) and representative HPC electrode tip location.

The effect of MS 0.9% NaCl injection on VNS-induced HPC theta rhythm

The effect of intra-septal injection of 0.9% NaCl on VNS-induced type II theta is shown in Fig 4. Fig 4A provides a representative example taken from one animal illustrating the effect of 0.9% NaCl micro-infusion into the MS on VNS-induced HPC type II theta in anesthetized rats. This figure also provides a corresponding power spectrum estimated from each data segment in pre- and post- injection time using the FFT (15 min). Before the MS microinjection of 0.9% NaCl, VNS-induced HPC theta rhythm in the power spectrum had a peak frequency 5.0 ± 0.1 Hz. At 15 min post-injection of 0.9% NaCl, VNS-elicited HPC theta (peak frequency 4.9 ± 0.2 Hz in power spectrum) had a mean power and frequency similar to VNS-induced

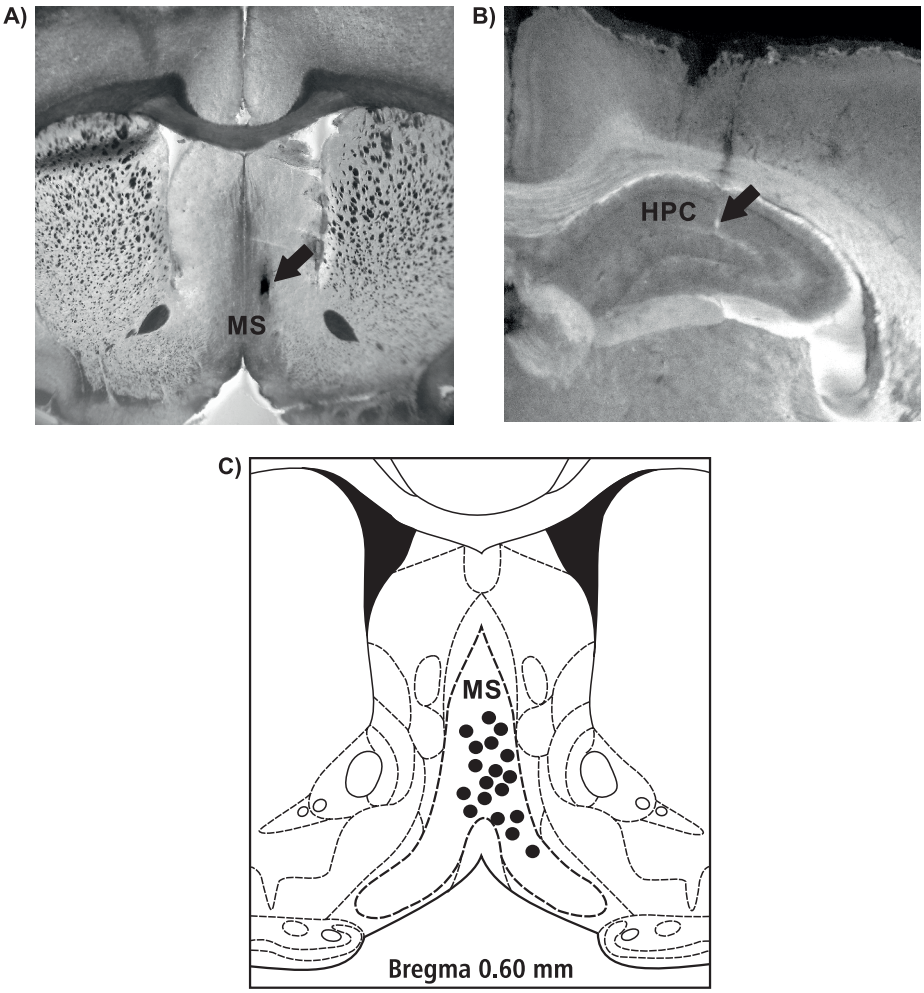

Fig 3. Microphotographs (A and B) and a diagrammatic reconstruction of representative locations of the injection sites in the medial septum in three representative rat preparations of each group (18 sites, C) and representative HPC electrode tip location.

https://doi.org/10.1371/journal.pone.0206532.g003

theta observed in the pre-injection segment ($p > 0.05$ for power, $p > 0.05$ for frequency, Mann-Whitney U test; Fig 4B, Table 2).

The effect of MS procaine injection on VNS-induced HPC theta rhythm

The effect of intra-septal injection of procaine on VNS-induced type II theta is shown in Fig 5. Fig 5A provides a representative example taken from one animal illustrating the effect of procaine microinjection into the MS on VNS-induced HPC type II theta rhythm in anesthetized rats. Fig 5A also provides a corresponding power spectrum estimated from each data segment in pre- and post- injection time using the FFT (at 15 and 60 min). Before the microinjection of procaine into the MS, VNS-induced HPC theta rhythm in the power spectrum had a peak frequency 4.6 ± 0.1 Hz. At 15 min post-injection, VNS no longer elicited HPC theta (absence of a peak in the power spectrum). At 60 min post-injection of procaine, VNS again elicited HPC theta with an power and frequency similar to the control, pre-injection conditions ($p > 0.05$ for power, $p > 0.05$ for frequency, Mann-Whitney U test; Fig 5B, Table 2).

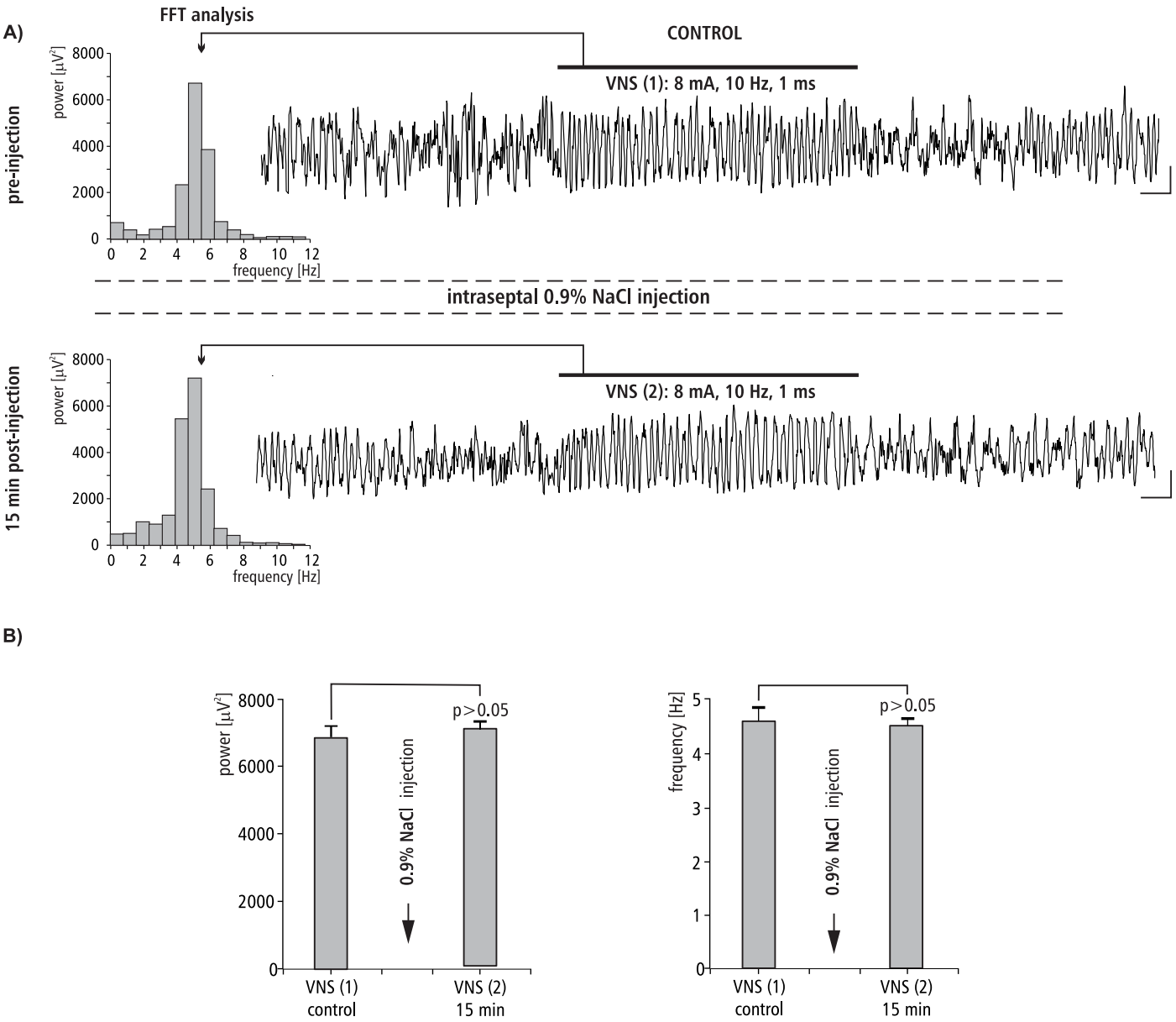

Fig 4. The effect of MS 0.9% NaCl injection on VNS-induced HPC field potential and related power-frequency (FFT) histogram. (A) VNS is marked with a horizontal line. The parameters of VNS are marked below this line. Arrows indicate the power-frequency histograms calculated from the analog examples of hippocampal field potentials taken pre-injection of 0.9% NaCl (control) and 15 min post-injection of 0.9% NaCl during 10 s VNS. Calibration: 1 s, 150 μV. (B) Statistical analysis (Mann-Whitney U test) of mean ± SEM power and frequency (VNS(1) vs VNS(2)).

https://doi.org/10.1371/journal.pone.0206532.g004

The effect of MS atropine injection on VNS-induced HPC theta rhythm

The effect of intra-septal injection of atropine on VNS-induced type II theta is shown in Fig 6. This figure provides a representative example taken from one animal illustrating the effect of atropine micro-infusion into the MS on VNS-induced HPC type II theta in anesthetized rats. Fig 6 also provides a corresponding power spectrum estimated from each data segment in pre- and post- injection time using the FFT (at 15 and 180 min). Before the microinjection of atropine into the MS control, VNS-induced HPC theta rhythm in the power spectrum had a peak frequency 4.9 ± 0.2 Hz. At 15 min post-injection, VNS no longer elicited HPC theta (absence

Table 2. Summated statistical details concerning power and frequency of VNS-induced theta rhythm after intraseptal injection of different agents (group I–group VI). Statistical analysis: Shapiro-Wilk and Kruskal-Wallis tests.

Number of VNS	Parameters of theta rhythm	Group					
		Group I	Group II	Group III	Group IV	Group V	Group VI
VNS(1) **control**	power (μV^2)	6882.0 ± 703.6	6786.0 ± 609.6	6911.8 ± 599.4	9392.6 ± 814.5	7003.9 ± 807.7	7488.0 ± 679.1
		$p > 0.05$	$p > 0.05$	$p > 0.05$	$p > 0.05$	$p > 0.05$	$p > 0.05$
	frequency (Hz)	5.0 ± 0.1	4.6 ± 0.1	4.9 ± 0.2	5.1 ± 0.1	5.2 ± 0.1	4.9 ± 0.2
		$p > 0.05$	$p > 0.05$	$p > 0.05$	$p > 0.05$	$p > 0.05$	$p > 0.05$
VNS(2)	power (μV^2)	7204.3 ± 633.8	No theta	No theta	No theta	6899.6 ± 747.5	7706.7 ± 728.2
		$p > 0.05$				$p > 0.05$	$p > 0.05$
	frequency (Hz)	4.9 ± 0.2				5.0 ± 0.1	5.0 ± 0.2
		$p > 0.05$				$p > 0.05$	$p > 0.05$
VNS(3)	power (μV^2)	---------	6211.0 ± 584.6	No theta	No theta	---------	9210.4 ± 812.7
			$p > 0.05$				$\mathbf{p < 0.01}$
	frequency (Hz)	---------	4.4 ± 0.2			---------	5.2 ± 0.1
			$p > 0.05$				$p > 0.05$

https://doi.org/10.1371/journal.pone.0206532.t002

of a peak in the power spectrum). At 180 min post-injection, atropine still completely abolished VNS-elicited HPC theta rhythm (absence of peak in power spectrum of the analog example taken at 180 min post-injection).

The effect of MS dicyclomine injection on VNS-induced HPC theta rhythm. The effect of intra-septal injection of M1 cholinergic antagonist dicyclomine on VNS-induced type II theta is shown in Fig 7. This figure provides a representative example taken from one animal illustrating the effect of dicyclomine micro-infusion into the MS on VNS-induced HPC type II theta in anesthetized rats. Fig 7 also provides a corresponding power spectrum estimated from each data segment in pre- and post- injection time using the FFT (at 15 and 180 min). Before the microinjection of dicyclomine into the MS, VNS-induced HPC theta rhythm in the power spectrum had a peak frequency 5.1 ± 0.1 Hz. At 15 min post-injection, VNS no longer elicited HPC theta (absence of a peak in the power spectrum). At 180 min post-injection, dicyclomine still completely abolished VNS elicited HPC theta rhythm (absence of a peak in the power spectrum of the analog example taken at 180 min post-injection).

The effect of MS gallamine injection on VNS-induced HPC theta rhythm

The effect of intraseptal injection of M2 cholinergic antagonist gallamine on VNS-induced type II theta is shown in Fig 8. Fig 8A provides a representative example taken from one animal illustrating the effect of gallamine microinjection into the MS on VNS-induced HPC type II theta in anesthetized rats. This figure also provides a corresponding power spectrum estimated from each data segment in pre- and post- injection time using the FFT (at 15 min). Before the microinjection of gallamine into the MS, VNS-induced HPC theta rhythm in the power spectrum had a peak frequency 5.2 ± 0.1 Hz. At 15 min post-injection of gallamine, VNS-elicited HPC theta (peak frequency 5.0 ± 0.1 Hz in the power spectrum) had a mean power and frequency similar to VNS-induced theta observed in the pre-injection segment ($p > 0.05$ for power, $p > 0.05$ for frequency, Mann-Whitney U test; Fig 8B, Table 2).

The effect of MS injection of McN-A343 on VNS-induced HPC theta rhythm

The effect of intraseptal injection of cholinergic M1 agonist McN-A343 on VNS-induced type II theta is shown in Fig 9. Fig 9A provides a representative example taken from one animal

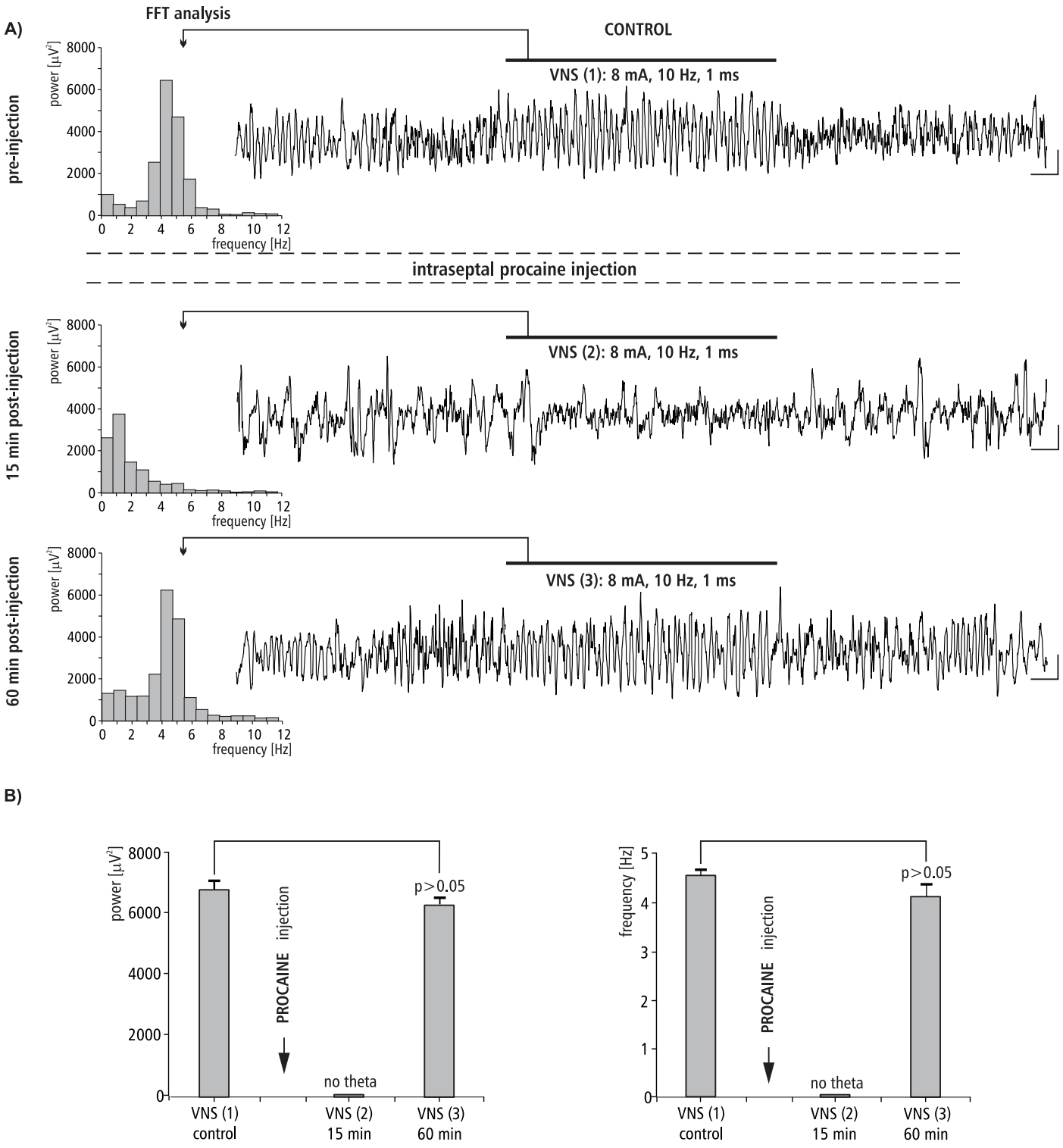

Fig 5. The effect of MS procaine injection on VNS-induced HPC field potential and related power-frequency (FFT) histogram. (A) VNS is marked with a horizontal line. The parameters of VNS are marked below this line. Arrows indicate the power-frequency histograms calculated from the analog examples of hippocampal field potentials taken pre-injection of procaine (control), 15 and 60 min post-injection of procaine during 10 s VNS. Calibration: 1s, 150 μV. (B) Statistical analysis (Mann-Whitney U test) of mean ± SEM power and frequency (VNS (1) vs VNS(3)).

https://doi.org/10.1371/journal.pone.0206532.g005

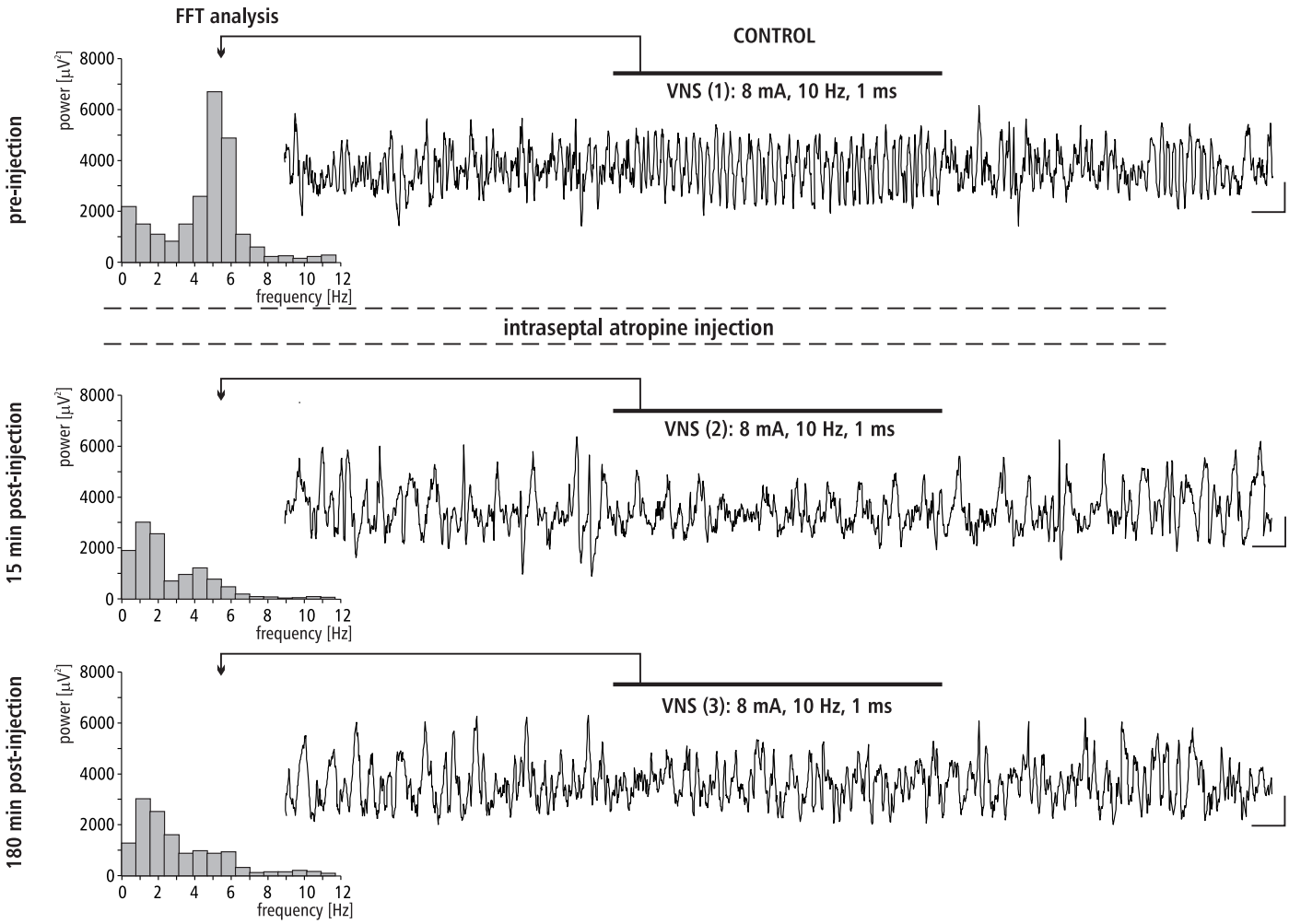

Fig 6. The effect of MS atropine injection on VNS-induced HPC field potential and related power-frequency (FFT) histogram. VNS is marked with a horizontal line. The parameters of VNS are marked below this line. Arrows indicate the power-frequency histograms calculated from the analog examples of hippocampal field potentials taken pre-injection of atropine (control), 15 and 180 min post-injection of atropine during 10 s VNS. Calibration: 1s, 150 μV.

https://doi.org/10.1371/journal.pone.0206532.g006

illustrating the effect of McN-A343 microinjection into the MS on VNS-induced HPC type II theta in anesthetized rats. This figure also provides a corresponding power spectrum estimated from each data segment in pre- and post- injection time using the FFT (at 15 min). Before the microinjection of McN-A343 into the MS, VNS-induced HPC theta rhythm in the power spectrum had a peak frequency 4.9 ± 0.2 Hz. At 60 min post-injection of McN-A343, VNS-elicited HPC theta (peak frequency 5.2 ± 0.1 Hz in power spectrum) had a similar mean frequency ($p > 0.05$, Mann-Whitney U test; Fig 9, Table 2). In contrast to the frequency, the power of VNS-induced HPC theta increased, especially 60 min post injection ($p < 0.01$, Mann-Whitney U test; Fig 9B, Table 2).

Discussion

The basic experimental model used in the present study to evaluate the central effect of VNS was HPC type II theta rhythm recorded in urethanized rats. We have recently provided the first evidence that, using different protocols and current pulse parameters, VNS produced a very well synchronized HPC type II theta [30].

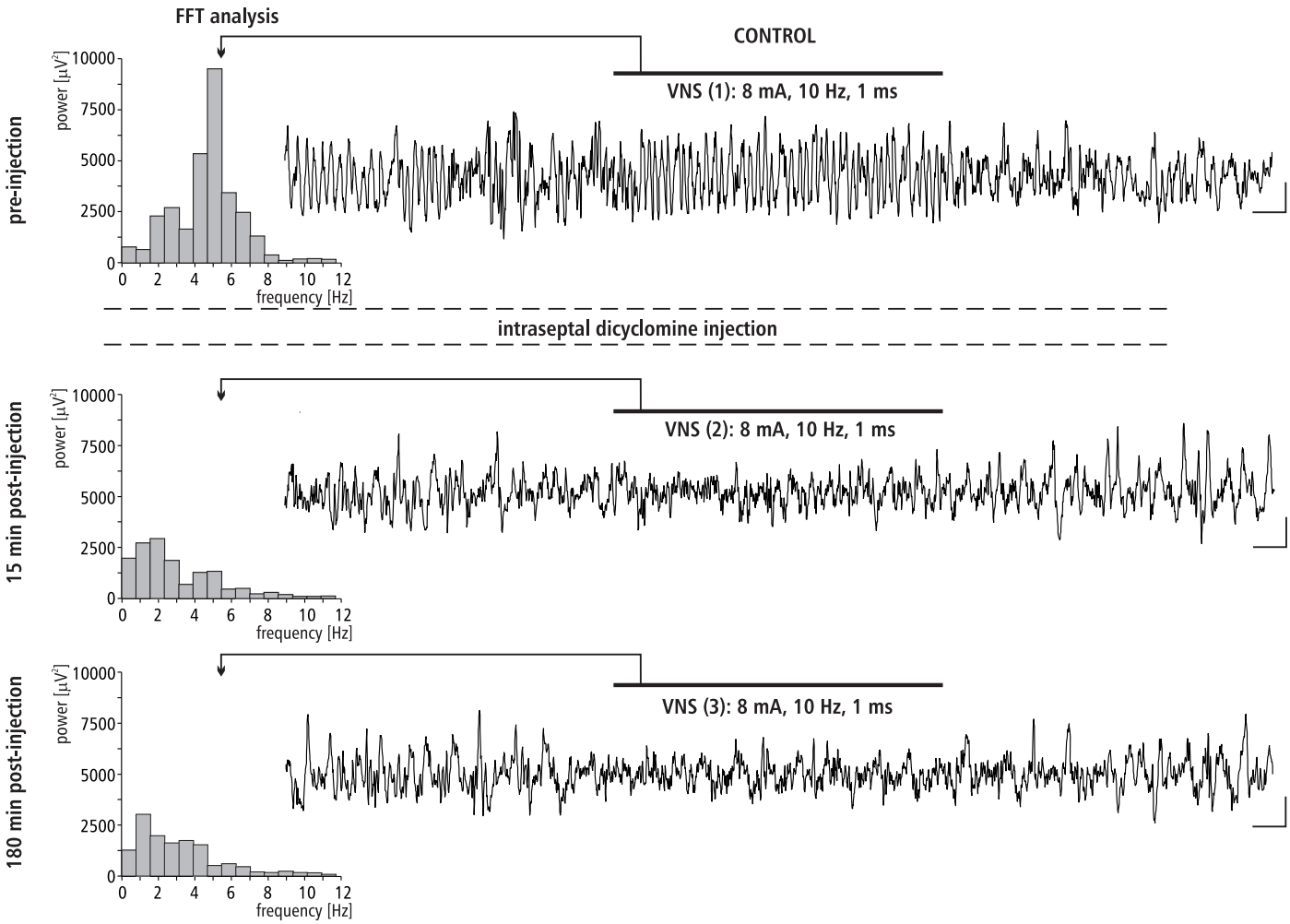

Fig 7. The effect of MS dicyclomine injection on VNS-induced HPC field potential and related power-frequency (FFT) histogram. VNS is marked with a horizontal line. The parameters of VNS are marked below this line. Arrows indicate the power-frequency histograms calculated from the analog examples of hippocampal field potentials taken pre-injection of dicyclomine (control), 15 and 180 min post-injection of dicyclomine during 10 s VNS. Calibration: 1s, 150 μV.

https://doi.org/10.1371/journal.pone.0206532.g007

The theta rhythm is considered to be a "fingerprint" of the limbic cortex [56]. Previous studies demonstrated that theta is involved in a number of physiological regulations, including LTP, learning and navigation, locomotor activity, and sensory-motor integration [57–65]. The studies also showed, both behaviorally and pharmacologically, that theta is not a homogenous field oscillation. In fact, two distinct types of theta rhythms have previously been distinguished: anesthetic-resistant and cholinergic-mediated type II theta at a frequency range of 3–6 Hz, and anesthetic-sensitive, probably serotonin-mediated type I theta (7–12 Hz), which is related to motor behaviors [38, 66–72]. This type of theta depends on the non-cholinergic pathway that arises from the neocortex and cingulate cortex and reaches the HPC via the entorhinal cortex [69].

Recently, Larsen et al. [73,74] using a model of freely moving rats (i.e. type I theta), demonstrated that VNS slowed theta rhythm and decreased its power. In contrast to Larsen et al. [73,74], in the present study, we tested type II theta rhythm which typically is observed in anesthetized rats. The generation of the HPC type II theta is determined by structures of pontine region, hypothalamus and basal forebrain which form the ascending brainstem hippocampal

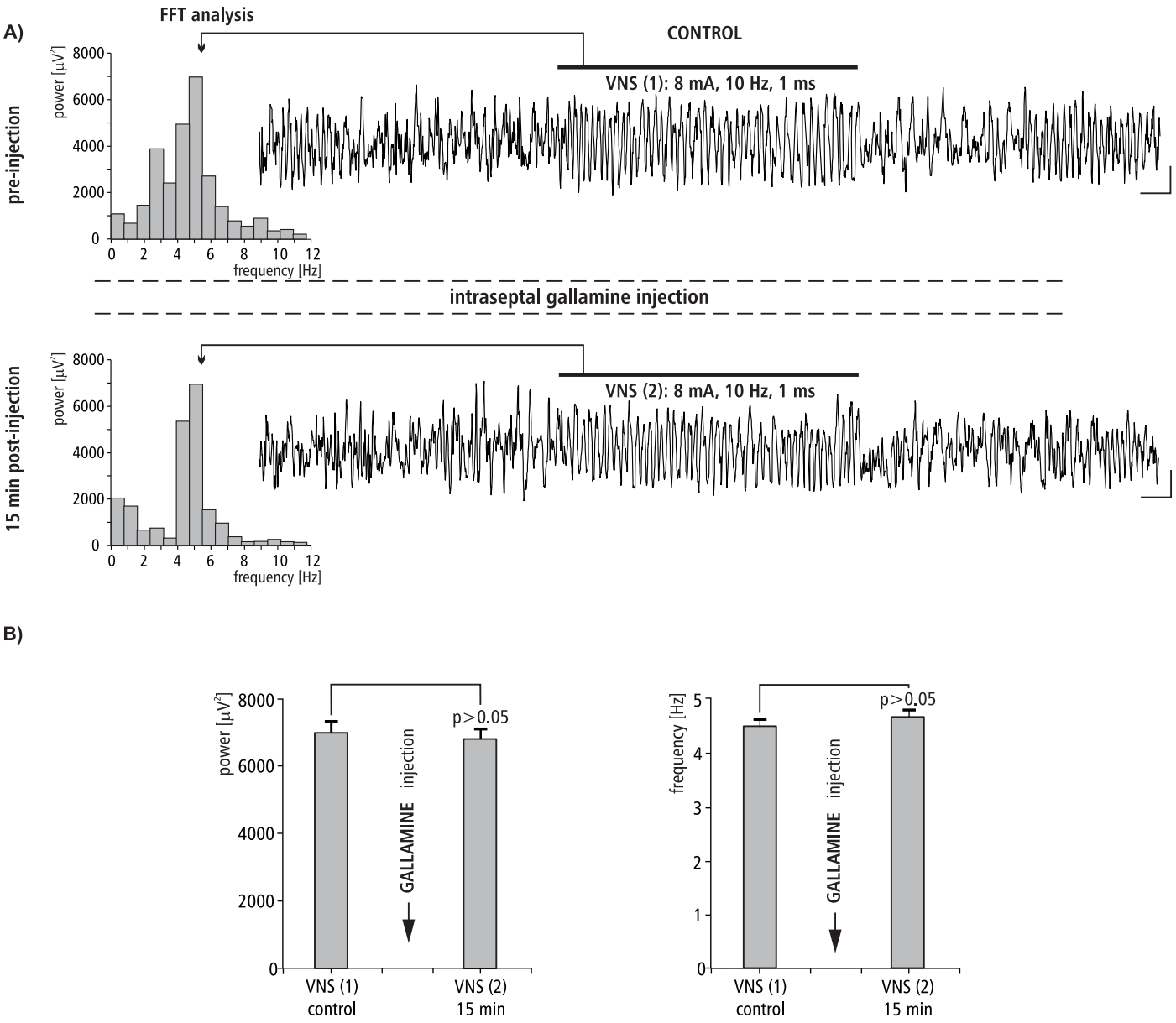

Fig 8. The effect of MS gallamine injection on VNS-induced HPC field potential and related power/frequency (FFT) histogram. (A) VNS was marked with a horizontal line. Parameters of VNS were marked below this line. Arrows indicate the power-frequency histograms calculated from analog examples of hippocampal field potentials taken pre-injection of gallamine (control) and 15 min post-injection of gallamine during 10 s VNS. Calibration: 1s, 150 μV. (B) Statistical analysis (Mann-Whitney U test) of mean ± SEM power and frequency (VNS(1) vs VNS(2)).

https://doi.org/10.1371/journal.pone.0206532.g008

synchronizing pathway [39,43,48,75,76]. The medial septum is considered to be a nodal point of this pathway [44]. On the basis of the above-mentioned data, it seems that in addition to the different model used and different VNS parameters and protocols applied previously [73,74], the difference in neuronal substrate between type II and type I theta could additionally determine a completely different response of HPC rhythmic field potential to VNS in the previous experiments [73,74]. Larsen et al. [73,74] had decisive arguments to suggest that VNS induces a decrease in hippocampal excitation since, in addition to the decrease in amplitude and power of type I theta rhythm, these authors observed decreased efficacy in synaptic

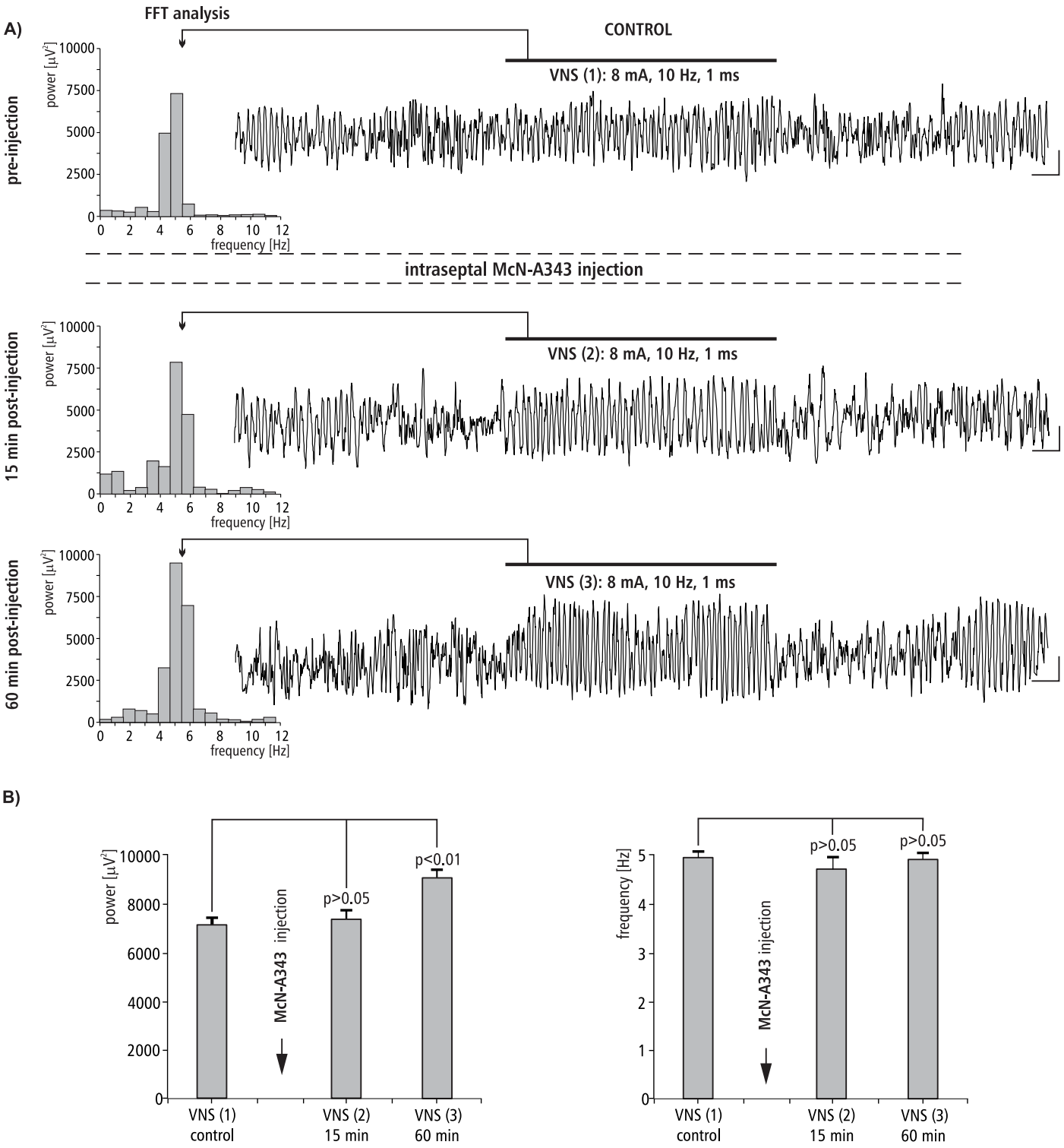

Fig 9. The effect of MS McN-A343 injection on VNS-induced HPC field potential and related power-frequency (FFT) histogram. (A) VNS is marked with a horizontal line. The parameters of VNS are marked below this line. Arrows indicate the power-frequency histograms calculated from analog examples of hippocampal field potentials taken pre-injection of McN-A343 (control), 15 and 60 min post-injection of McN-A343 during 10 s VNS. Calibration: 1 s, 150 μV. (B) Statistical analysis (Mann-Whitney U test) of mean ± SEM power and frequency (VNS(1) vs VNS(2), and VNS(1) vs VNS(3)).

https://doi.org/10.1371/journal.pone.0206532.g009

transmission. Considering our data concerning type II theta, which appears when the animal is still or anesthetized, we would not go so far as to suggest that VNS induces inhibition of the hippocampal neuronal network. Quite the opposite. The presented data actually indicates the excitation of the hippocampal formation during VNS, as previously suggested [30]. This suggestion is also supported by earlier findings that VNS potentiates hippocampal LTP and enhances hippocampal synaptic transmission in freely moving and anesthetized rats [19,20,23].

The medial septum, is widely accepted to be the pivotal extrinsic regulator of theta rhythm occurring in the limbic system [43,48,77]. The main function of the MS/vDBB is the distribution of inputs to the cingulate cortex, entorhinal cortex, and hippocampal formation, i.e. limbic structures in which well synchronized, local theta field potentials are observed. Rhythmic outputs from the medial septum area act as a "pacemaker" for those structures, inducing theta rhythm [38,39,48,50,67,76,78–82].

In the light of the above-presented data, new and important findings regarding the neuronal substrate underlying HPC type II theta rhythm emerged from the present study. The results of the second experiment, that temporal inactivation of the MS by the local anesthetic procaine reversibly abolishes VNS-induced HPC theta, clearly demonstrate that medial septum integrates not only central inputs from the brainstem synchronizing pathway which underlies the production of HPC type II theta rhythm, but also input from the vagal nerve.

The pharmacological profile of the MS involved in the VNS effect on HPC rhythmic field potentials was evaluated in the remaining experiments described. The experiments conducted in the group III and IV, with use of the MS injection of atropine, the nonselective muscarinic receptor antagonist and dicyclamine, the selective M1 antagonist, suggest that the M1 receptor subtype is involved in the medial-septal mediation of the VNS effect on hippocampal field potential since both agents irreversibly abolished VNS-elicited HPC theta. This suggestion was proved in the next experiments conducted with use of gallamine, the selective antagonist of M2 receptors. Specifically, the MS injection of this agent did not affect the HPC theta rhythm induced by VNS. The definitive confirmation of M1 receptor profile of VNS-induced type II theta was provided in the experiment with the use of McN-A343. This selective M1 receptor agonist was found to enhance the VNS-induced HPC theta power. The described cholinergic profile of VNS-induced type II theta rhythm supports earlier pharmacological findings concerning this type of theta [38,50,67,83–85].

Although the involvement of the muscarinic M1 receptor subtype in the central pharmacological mechanism underlying VNS-induced HPC type II theta was proved in the present experiments, the possible participation of other noncholinergic receptors cannot be discounted. Previous electrophysiological and neurochemical data suggested that the modulatory effect of VNS on hippocampal LTP may involve the central noradrenergic systems. It was earlier pointed out that VNS potentiates noradrenaline (NE) release in the hippocampus [8,17,18] and NE was also demonstrated to increase the discharge rate of HPC pyramidal and granular cells [86,87]. Interestingly, it was also shown that blockade of the dorsal ascending noradrenergic bundle abolished septal elicitation of HPC theta rhythm [88]. On the other hand, NE has never been demonstrated to affect hippocampal theta-related cells, which underlies this field potential [67]. Additionally, the bath perfusion of the hippocampal formation slices with NE did not elicit theta oscillation and did not even alter the production of cholinergic-induced theta rhythm in the HPC slice preparations [89].

Finally, one more issue should be addressed. The other possible explanation for the observed effect of VNS on HPC type II theta rhythm is that VNS may cause changes in peripherally released stress-related hormones, which, in turn, may affect hippocampal function through a mechanism not related to the medial septal area. For example, corticosterone was

earlier demonstrated to induce the release of hippocampal acetylcholine [90] leading to the increase of the theta amplitude [91]. However, it should also be pointed out that the release of the corticosterone takes a relatively slow time and VNS-induced theta rhythm appeared in the present study immediately during stimulation.

In summary, the present data provide the first evidence for the role of the medial septum in the mechanism of the effect of VNS on hippocampal formation type II theta rhythm in rats. In addition, the present experiments, with the use of cholinergic muscarinic agonist and antagonists, demonstrated for the first time the involvement of muscarinic M1 receptor subtype in the medial septal mediation of VNS-induced HPC theta.

Author Contributions

Conceptualization: Adam Broncel, Jan Konopacki.

Formal analysis: Renata Bocian.

Investigation: Adam Broncel, Renata Bocian, Paulina Kłos-Wojtczak.

Methodology: Adam Broncel, Renata Bocian, Paulina Kłos-Wojtczak.

Supervision: Adam Broncel, Jan Konopacki.

Visualization: Renata Bocian.

Writing – original draft: Jan Konopacki.

Writing – review & editing: Renata Bocian.

References

1. Aalbers M, Vles J, Klinkenberg S, Hoogland G, Majoie M, Rijkers K. Animal models for vagus nerve stimulation in epilepsy. Exp Neurol 2011; 230:167–75. https://doi.org/10.1016/j.expneurol.2011.04.014 PMID: 21565191
2. Ben-Menachem E. Vagus-nerve stimulation for the treatment of epilepsy. Lancet Neurol 2002; 1:477–82. PMID: 12849332
3. DeGiorgio CM, Schachter SC, Handforth A, Salinsky M, Thompson J, Uthman B, et al. Prospective long-term study of vagus nerve stimulation for the treatment of refractory seizures. Epilepsia 2000; 41:1195–200. PMID: 10999559
4. Howland RH. Vagus nerve stimulation. Curr Behav Neurosci Rep 2014; 1:64–73. https://doi.org/10.1007/s40473-014-0010-5 PMID: 24834378
5. Krahl SE, Senanayake SS, Handforth A. Right-sided vagus nerve stimulation reduces generalized seizure severity in rats as effectively as left-sided. Epilepsy Res 2003; 56:1–4. PMID: 14529948
6. Sjögren MJ, Hellström PT, Jonsson MA, Runnerstam M, Silander HC, Ben-Menachem E. Cognition-enhancing effect of vagus nerve stimulation in patients with Alzheimer's disease: a pilot study. J Clin Psychiatry 2002; 63:972–80. PMID: 12444809
7. Krahl SE, Senanayake SS, Pekary AE, Sattin A. Vagus nerve stimulation (VNS) is effective in a rat model of antidepressant action. J Psychiatr Res 2004; 38:237–40. https://doi.org/10.1016/j.jpsychires.2003.11.005 PMID: 15003428
8. Manta S, El Mansari M, Debonnel G, Blier P. Electrophysiological and neurochemical effects of long-term vagus nerve stimulation on the rat monoaminergic systems. Int J Neuropsychopharmacol 2013; 16:459–70. https://doi.org/10.1017/S1461145712000387 PMID: 22717062
9. Smucny J, Visani A, Tregellas JR. Could vagus nerve stimulation target hippocampal hyperactivity to improve cognition in schizophrenia? Front Psychiatry 2015; 6:43. https://doi.org/10.3389/fpsyt.2015.00043 PMID: 25852579
10. Hord ED, Evans MS, Mueed S, Adamolekun B, Naritoku DK. The effect of vagus nerve stimulation on migraines. J Pain 2003; 4:530–4. PMID: 14636821
11. Straube A, Ellrich J, Eren O, Blum B, Ruscheweyh R. Treatment of chronic migraine with transcutaneous stimulation of the auricular branch of the vagal nerve (auricular t-VNS): a randomized, monocentric

clinical trial. J Headache Pain 2015; 16:543. https://doi.org/10.1186/s10194-015-0543-3 PMID: 26156114

12. Bonaz B, Picq C, Sinniger V, Mayol JF, Clarençon D. Vagus nerve stimulation: from epilepsy to the cholinergic anti-inflammatory pathway. Neurogastroenterol Motil 2013; 25:208–21. https://doi.org/10.1111/nmo.12076 PMID: 23360102
13. Xiang YX, Wang WX, Xue Z, Zhu L, Wang SB, Sun ZH. Electrical stimulation of the vagus nerve protects against cerebral ischemic injury through an anti-infammatory mechanism. Neural Regen Res 2015; 10:576–82. https://doi.org/10.4103/1673-5374.155430 PMID: 26170817
14. Smith DC, Modglin AA, Roosevelt RW, Neese SL, Jensen RA, Browning RA, et al. Electrical stimulation of the vagus nerve enhances cognitive and motor recovery following moderate fluid percussion injury in the rat. J Neurotraum 2005; 22:1485–502.
15. Rizzo P, Beelke M, De Carli F, Canovaro P, Nobili L, Robert A, et al. Chronic vagus nerve stimulation improves alertness and reduces rapid eye movement sleep in patients affected by refractory epilepsy. Sleep 2003; 26:607–11. PMID: 12938816
16. Peña DF, Childs JE, Willett S, Vital A, McIntyre CK, Kroener S. Vagus nerve stimulation enhances extinction of conditioned fear and modulates plasticity in the pathway from the ventromedial prefrontal cortex to the amygdala. Front Behav Neurosci 2014; 8:327. https://doi.org/10.3389/fnbeh.2014.00327 PMID: 25278857
17. Raedt R, Clinckers R, Mollet L, Vonck K, El Tahry R, Wyckhuys T, et al. Increased hippocampal noradrenaline is a biomarker for efficacy of vagus nerve stimulation in a limbic seizure model. J Neurochem 2011; 117:461–9. https://doi.org/10.1111/j.1471-4159.2011.07214.x PMID: 21323924
18. Roosevelt RW, Smith DC, Clough RW, Jensen RA, Browning RA. Increased extracellular concentrations of norepinephrine in cortex and hippocampus following vagus nerve stimulation in the rat. Brain Res 2006; 1119:124–32. PMID: 16962076
19. Biggio F, Gorini G, Utzeri C, Olla P, Marrosu F, Mocchetti I, et al. Chronic vagus nerve stimulation induces neuronal plasticity in the rat hippocampus. Int J Neuropsychopharmacol 2009; 12:1209–21. https://doi.org/10.1017/S1461145709000200 PMID: 19309534
20. Zuo Y, Smith DC, Jensen RA. Vagus nerve stimulation potentiates hippocampal LTP in freely-moving rats. Physiol Behav 2007; 90:583–9. https://doi.org/10.1016/j.physbeh.2006.11.009 PMID: 17207505
21. Clark KB, Naritoku DK, Smith DC, Browning RA, Jensen RA. Enhanced recognition memory following vagus nerve stimulation in human subjects. Nat Neurosci 1999; 2:94–8. https://doi.org/10.1038/4600 PMID: 10195186
22. Ghacibeh GA, Shenker JI, Shenal B, Uthman BM, Heilman KM. The influence of vagus nerve stimulation on memory. Cogn Behav Neurol 2006; 19:119–22. https://doi.org/10.1097/01.wnn.0000213908.34278.7d PMID: 16957488
23. Ura H, Sugaya Y, Ohata H, Takumi I, Sadamoto K, Shibasaki T, et al. Vagus nerve stimulation induced long-lasting enhancement of synaptic transmission and decreased granule cell discharge in the hippocampal dentate gyrus of urethane-anesthetized rats. Brain Res 2013; 1492:63–71. https://doi.org/10.1016/j.brainres.2012.11.024 PMID: 23183039
24. Boyce R, Glasgow SD, Williams S, Adamantidis A. Causal evidence for the role of REM sleep theta rhythm in contextual memory consolidation. Science 2016; 352:812–6. https://doi.org/10.1126/science.aad5252 PMID: 27174984
25. Buzsáki G, Moser EI. Memory, navigation and theta rhythm in the hippocampal-entorhinal system. Nat Neurosci 2013; 16:130–8. https://doi.org/10.1038/nn.3304 PMID: 23354386
26. Lopes da Silva FH. Neural mechanisms underlying brain waves: from neural membranes to networks. Electroenceph Clin Neurophysiol 1991; 79:81–93. PMID: 1713832
27. Steriade M, Gloor P, Llinás RR, Lopes de Silva FH, Mesulam MM. Report of IFCN Committee on Basic Mechanisms. Basic mechanisms of cerebral rhythmic activities. Electroencephalogr Clin Neurophysiol 1990; 76:481–508. PMID: 1701118
28. Yamaguchi Y, Aota Y, Sato N, Wagatsuma H, Wu Z. Synchronization of neural oscillations as a possible mechanism underlying episodic memory: a study of theta rhythm in the hippocampus. J Integr Neurosci 2004; 3:143–57. PMID: 15285052
29. Watson BO, Buzsáki G. Sleep, Memory & Brain Rhythms. Daedalus 2015; 144:67–82. https://doi.org/10.1162/DAED_a_00318 PMID: 26097242
30. Broncel A, Bocian R, Kłos-Wojtczak P, Konopacki J. Vagus nerve stimulation produces a hippocampal formation theta rhythm in anesthetized rats. Brain Res 2017; 1675:41–50. https://doi.org/10.1016/j.brainres.2017.08.030 PMID: 28867480
31. Paton JF, Li YW, Deuchars J, Kasparov S. Properties of solitary tract neurons receiving inputs from the sub-diaphragmatic vagus nerve. Neuroscience 2000; 95:141–53. PMID: 10619470

32. Brog JS, Salyapongse A, Deutch AY, Zahm DS. The patterns of afferent innervation of the core and shell in the "accumbens" part of the rat ventral striatum: immunohistochemical detection of retrogradely transported fluoro-gold. J Comp Neurol 1993; 338:255–278. https://doi.org/10.1002/cne.903380209 PMID: 8308171

33. Halsell CB. Organization of parabrachial nucleus efferents to the thalamus and amygdala in the golden hamster. J Comp Neurol 1992; 317:57–78. https://doi.org/10.1002/cne.903170105 PMID: 1374087

34. Peyron C, Luppi PH, Fort P, Rampon C, Jouvet M. Lower brainstem catecholamine afferents to the rat dorsal raphe nucleus. J Comp Neurol 1996; 364:402–413. PMID: 8820873

35. Ter Horst GJ, de Boer P, Luiten PG, van Willigen JD. Ascending projections from the solitary tract nucleus to the hypothalamus. A Phaseolus vulgaris lectin tracing study in the rat. Neuroscience 1989; 31:785–97. PMID: 2594200

36. Van Bockstaele EJ, Saunders A, Telegan P, Page ME. Localization of mu-opioid receptors to locus coeruleus-projecting neurons in the rostral medulla: morphological substrates and synaptic organization. Synapse 1999; 34:154–67. https://doi.org/10.1002/(SICI)1098-2396(199911)34:2<154::AID-SYN8>3.0.CO;2-C PMID: 10502314

37. Castle M, Comoli E, Loewy AD. Autonomic brainstem nuclei are linked to the hippocampus. Neuroscience 2005; 134:657–69. https://doi.org/10.1016/j.neuroscience.2005.04.031 PMID: 15975727

38. Bland BH. The physiology and pharmacology of hippocampal formation theta rhythms. Prog. Neurobiol 1986; 26:1–54. PMID: 2870537

39. Bland BH. The medial septum: Node of the ascending brainstem hippocampal synchronizing pathways. In: Numan R, editor. The behavioral neuroscience of the septal region, New York: Springer-Verlag; 2000, p. 115–145.

40. Buño W Jr, Garcia-Sanchez JL, Garcia-Austt E. Reset of hippocampal rhythmical activities by afferent stimulation. Brain Res Bull 1978; 3:21–8. PMID: 630419

41. Buzsáki G, Leung LW, Vanderwolf CH. Cellular bases of hippocampal EEG in the behaving rat. Brain Res 1983; 287:139–71. PMID: 6357356

42. Shapiro ML, Findling R L, Olton D S, Gage FH, Stenevi I-J, Bjiirklund A. Hippocampal unit activity altered by lesions of the fimbria-fornix in rats. Soc Neurosci Abstr 1983; 13:87.

43. Bland BH, Oddie SD. Anatomical, electrophysiological and pharmacological studies of ascending brainstem hippocampal synchronizing pathways. Neurosci Biobehav Rev 1998; 22:259–73. PMID: 9579317

44. Bland BH, Oddie SD, Colom LV. Mechanisms of neural synchrony in the septohippocampal pathways underlying hippocampal theta generation. J Neurosci 1999; 19:3223–37. PMID: 10191335

45. Brunello N, Cheney DL. The septal-hippocampal cholinergic pathway: role in antagonism of pentobarbital anesthesia and regulation by various afferents. J Pharmacol Exp Ther 1981; 219:489–95. PMID: 6793716

46. Fibiger HC. The organization and some projections of cholinergic neurons of the mammalian forebrain. Brain Res 1982; 257:327–88. PMID: 6756546

47. Storm-Mathisen J, Woxen Opsahl M. Asparate and/or glutamate may be transmitters in hippocampal efferents to septum and hypothalamus. Neurosci Lett 1978; 9:65–70. PMID: 19605195

48. Vertes RP, Kocsis B. Brainstem-diencephalo-septohippocampal systems controlling the theta rhythm of the hippocampus. Neuroscience 1997; 8:893–926.

49. Goutagny R, Luppi PH, Salvert D, Lapray D, Gervasoni D, Fort P. Role of the dorsal paragigantocellular reticular nucleus in paradoxical (rapid eye movement) sleep generation: a combined electrophysiological and anatomical study in the rat. Neuroscience 2008; 152:849–57. https://doi.org/10.1016/j.neuroscience.2007.12.014 PMID: 18308473

50. Lee MG, Chrobak JJ, Sik A, Wiley RG, Buzsáki G. Hippocampal theta activity following selective lesion of the septal cholinergic systems. Neuroscience 1994; 2:1033–1047.

51. Broncel A, Bocian R, Kłos-Wojtczak P, Konopacki J. Intraseptal procaine injection abolishes theta rhythm induced by vagal nerve stimulation. Acta Neurobiol Exp 2017; 77: LXXXIX, P1.94.

52. Kłos-Wojtczak P, Broncel A, Bocian R, Konopacki J. Medial-septal cholinergic mediation of hippocampal theta rhythm induced by vagal stimulation in rats. Acta Neurobiol Exp 2017; 77: LXXXVIII, P1.92.

53. Paxinos G, Watson C. The Rat Brain in Stereotaxic Coordinates. 7th ed. San Diego: Academic Press; 2014.

54. Oddie SD, Stefanek W, Kirk IJ, Bland BH. Intraseptal procaine abolishes hypothalamic stimulation-induced wheel-running and hippocampal theta field activity in rats. J Neurosci 1996; 16:1948–56. PMID: 8774461

55. Li S, Topchiy I, Kocsis B. The effect of atropine administered in the medial septum or hippocampus on high- and low-frequency theta rhythms in the hippocampus of urethane anesthetized rats. Synapse 2007; 61:412–9. https://doi.org/10.1002/syn.20388 PMID: 17372965

56. Lopes da Silva FH. The rhythmic slow activity (theta) of the limbic cortex: Mechanisms of generation, models and functional implications. In: Bullock TH, Basar E, editors. Induced Rhythms in the Brain, Cambridge, MA: MIT Press; 1992, p.83–102.

57. Buzsáki G. Theta oscillations in the hippocampus. Neuron 2002; 33:325–40. PMID: 11832222

58. Leung LS. Generation of theta and gamma rhythms in the hippocampus. Neurosci Biobehav Rev 1998; 22:275–90. PMID: 9579318

59. Pavlides C, Greenstein YJ, Grudman M, Winson J. Long-term potentiation in the dentate gyrus is induced preferentially on the positive phase of theta-rhythm. Brain Res 1988; 439:383–7. PMID: 3359196

60. Huerta PT, Lisman JE. Bidirectional synaptic plasticity induced by a single burst during cholinergic theta oscillation in CA1 in vitro. Neuron 1995; 15:1053–63. PMID: 7576649

61. Hasselmo ME, Hay J, Ilyn M, Gorchetchnikov A. Neuromodulation, theta rhythm and rat spatial navigation. Neural Netw 2002; 15:689–707. PMID: 12371520

62. Winson J. Loss of hippocampal theta rhythm results in spatial memory deficit in the rat. Science 1978; 201:160–3. PMID: 663646

63. Bland BH, Jackson J, Derrie-Gillespie D, Azad T, Rickhi A, Abriam J. Amplitude, frequency, and phase analysis of hippocampal theta during sensorimotor processing in a jump avoidance task. Hippocampus 2006; 16:673–81. https://doi.org/10.1002/hipo.20210 PMID: 16858673

64. Oddie SD, Bland BH. Hippocampal formation theta activity and movement selection. Neurosci Biobehav Rev 1998; 22:221–31. PMID: 9579313

65. Bland BH, Oddie SD. Theta band oscillation and synchrony in the hippocampal formation and associated structures: the case for its role in sensorimotor integration. Behav Brain Re. 2001; 127:119–36.

66. Vanderwolf CH. Hippocampal electrical activity and voluntary movement in the rat. Electroenceph Clin Neurophysiol 1969; 26:407–418. PMID: 4183562

67. Bland BH, Colom LV. Extrinsic and intrinsic properties underlying oscillation and synchrony in limbic cortex. Prog Neurobiol 1993; 41:157–208. PMID: 8332751

68. Sainsbury R.S. Hippocampal theta: a sensory-inhibition theory of function. Neurosci. Biobehav Rev 1998; 22:237–241. PMID: 9579315

69. Lopes da Silva FH, Witter MP, Boeijinga PH, Lohman AH. Anatomic organization and physiology of the limbic cortex. Physiol Rev 1990; 70:453–511. https://doi.org/10.1152/physrev.1990.70.2.453 PMID: 2181500

70. Crooks R, Jackson J, Bland BH. Dissociable pathways facilitate theta and non-theta states in the median raphe-septo-hippocampal circuit. Hippocampus. 2012; 22:1567–76. https://doi.org/10.1002/hipo.20999 PMID: 22180148

71. Vanderwolf CH, Baker GB. Evidence that serotonin mediates non-cholinergic neocortical low voltage fast activity, non-cholinergic hippocampal rhythmical slow activity and contributes to intelligent behavior. Brain Res 1986; 374:342–356. PMID: 2941111

72. Sainsbury RS. Type 2 theta in the guinea pig and the cat. In: Buzsáki G, Vanderwolf CH, editors. Electrical activity of the archicortex, Budapest: Akademiai Kiado; 1985, p. 11–22.

73. Larsen LE, Wadman WJ, Marinazzo D, van Mierlo P, Delbeke J, Daelemans S, et al. Vagus nerve stimulation applied with a rapid cycle has more profound influence on hippocampal electrophysiology than a standard cycle. Neurotherapeutics 2016; 13:592–602. https://doi.org/10.1007/s13311-016-0432-8 PMID: 27102987

74. Larsen LE, Wadman WJ, van Mierlo P, Delbeke J, Grimonprez A, Van Nieuwenhuyse B, et al. Modulation of hippocampal activity by vagus nerve stimulation in freely moving rats. Brain Stimul 2016; 9:124–132. https://doi.org/10.1016/j.brs.2015.09.009 PMID: 26481670

75. Oddie SD, Bland BH, Colom LV, Vertes RP. The midline posterior hypothalamic region comprises a critical part of the ascending brainstem hippocampal synchronizing pathway. Hippocampus 1994; 4:454–473. https://doi.org/10.1002/hipo.450040408 PMID: 7874237

76. Vertes RP. An analysis of ascending brainstem systems involved in hippocampal synchronization and desynchronization. J Neurophysiol 1981; 46:1140–1159. https://doi.org/10.1152/jn.1981.46.5.1140 PMID: 7299451

77. Pignatelli M, Beyeler A, Leinekugel X. Neural circuits underlying the generation of theta oscillations. J Physiol Paris 2012; 106:81–92. https://doi.org/10.1016/j.jphysparis.2011.09.007 PMID: 21964249

78. Kang D, Ding M, Topchiy I, Shifflett L, Kocsis B. Theta-rhythmic drive between medial septum and hippocampus in slow-wave sleep and microarousal: a Granger causality analysis. J Neurophysiol 2015; 114:2797–803. https://doi.org/10.1152/jn.00542.2015 PMID: 26354315

79. Monmaur P, Breton P. Elicitation of hippocampal theta by intraseptal carbachol injection in freely moving rats. Brain Res 1991; 544:150–5. PMID: 1855135

80. Petsche H, Gogolak G, Van Zwieten PA. Rhytmicity of septal cells discharges at various level of reticular excitation. Electroenceph Clin Neurophysiol 1965; 19:25–33. PMID: 14325384

81. Smythe JW, Colom LV, Bland BH. The extrinsic modulation of hippocampal theta depends on the coactivation of cholinergic and GABA-ergic medial septal inputs Neurosci Behav Rev 1992; 16:289–308.

82. Stewart M, Fox SE. Two populations of rhythmically bursting neurons in rat medial septum are revealed by atropine. J Neurophysiol 1989; 61:982–993. https://doi.org/10.1152/jn.1989.61.5.982 PMID: 2723736

83. Gołębiewski H, Eckersdorf B, Konopacki J. Septal cholinergic mediation of hippocampal theta in the cat. Brain Res Bull 2002; 58:323–35. PMID: 12128160

84. Oddie SD, Kirk IJ, Whishaw IQ, Bland BH. Hippocampal formation is involved in movement selection: evidence from medial septal cholinergic modulation and concurrent slow-wave (theta rhythm) recording. Behav Brain Res 1997; 88:169–80. PMID: 9404626

85. Yamasaki N, Stanford IM, Hall SD, Woodhall GL. Pharmacologically induced and stimulus evoked rhythmic neuronal oscillatory activity in the primary motor cortex in vitro. Neuroscience 2008; 151:386–95. https://doi.org/10.1016/j.neuroscience.2007.10.021 PMID: 18063484

86. Knight J, Harley CW. Idazoxan increases perforant path-evoked EPSP slope paired pulse inhibition and reduces perforant path-evoked population spike paired pulse facilitation in rat dentate gyrus. Brain Res 2006; 1072:36–45. https://doi.org/10.1016/j.brainres.2005.12.020 PMID: 16426582

87. Manta S, Dong J, Debonnel G, Blier P. Enhancement of the function of rat serotonin and norepinephrine neurons by sustained vagus nerve stimulation. J Psychiatry Neurosci 2009; 34:272–80. PMID: 19568478

88. McNaughton N, Kelly PH, Gray JA. Unilateral blockade of the dorsal ascending noradrenergic bundle and septal elicitation of hippocampal theta rhythm. Neurosci Lett 1980; 18:67–72. PMID: 6820484

89. Konopacki J. Theta-like activity in the limbic cortex in vitro. Neurosci Biobehav Rev 1998; 22:311–23. PMID: 9579321

90. Gilad GM, Rabey JM, Tizabi Y, Gilad VH. Age-dependent loss and compensatory changes of septohippocampal cholinergic neurons in two rat strains differing in longevity and response to stress. Brain Res 1987; 436:311–22. PMID: 3435831

91. Murphy D, Costall B, Smythe JW. Regulation of hippocampal theta activity by corticosterone: opposing functions of mineralocorticoid and glucocorticoid receptors. Brain Res Bull 1998; 45:631–5. PMID: 9566508

Brain Research Bulletin 140 (2018) 402–410

Contents lists available at ScienceDirect

Brain Research Bulletin

journal homepage: www.elsevier.com/locate/brainresbull

Research report

Some technical issues of vagal nerve stimulation. An approach using a hippocampal formation theta rhythm

Adam Broncel[a], Renata Bocian[b,*], Paulina Kłos-Wojtczak[a,b], Jan Konopacki[b]

[a] Neuromedical, Natolin 15, 92-701 Łódź, Poland
[b] Department of Neurobiology, Faculty of Biology and Environmental Protection, The University of Lodz, Pomorska St. No 141/143, 90-236 Łódź, Poland

ARTICLE INFO

Keywords:
Type II theta rhythm
Cranial nerves
Limbic system
Cuff electrode
Fork electrode

ABSTRACT

Previously, we have demonstrated that hippocampal (HPC) theta rhythm can be produced, depending on current intensity, directly during vagal nerve stimulation (VNS) or with a time delay following stimulation. This suggests that theta EEG pattern can also be used as a bio-indicator of the efficiency of VNS. In the present study, we focused on three specific, technical issues related to the stimulation procedure of the vagal nerve: i/does the type of the electrode used for VNS and the technique of its implantation affect the parameters of the HPC theta rhythm? ii/does the type of electrode used determine the current intensity threshold of VNS-induced HPC theta? iii/is the repeatability of the VNS effect determined by the type of electrode used?

We demonstrated that a platinum-iridium cuff electrode offers some important advantages over a tungsten electrode. Firstly, despite some possible mechanical and compression nerve damage related to permanent contact with the vagal nerve, it offers a lower current intensity threshold for inducing theta oscillations. Secondly, and most importantly, the cuff electrode offers repeatability of the VNS effect on the HPC theta rhythm. However, one disadvantage of using this type of an electrode is that the permanent pressure on the vagal nerve by the cuff itself may decrease the amplitude of the investigated field potential.

1. Introduction

Vagal nerve stimulation (VNS) refers to any technique that stimulates the vagal nerve, including manual or electrical stimulation. The development of the VNS technique began in the 19th century, when an American neurologist James Corning observed that manual massage and compression of the carotid artery in the cervical region of the neck could suppress seizures (Lanska, 2002). Later, the same author applied a “carotid fork” for electrical stimulation of the vagal nerve to treat a patient with epilepsy. Although Corning reported that this form of VNS was dramatically effective for seizure-suppression, it was not widely accepted by his contemporaries and was largely forgotten about for a century (Lanska, 2002). Over time, VNS has become more and more widespread in medical practice. Nowadays, VNS is used not only for the treatment of epilepsy but also for bipolar disorders (Cimpianu et al., 2017), treatment-resistant anxiety disorders (Howland et al., 2011), Alzheimer’s disease (Merrill et al., 2006), traumatic brain injury (Neren et al., 2016), strokes (Hays et al., 2016), cluster headaches (Mauskop, 2005), chronic refractory migraines (Mauskop, 2005), central inflammation (Xiang et al., 2015) and heart failure (De Ferrari and Schwartz, 2011).

The vagal nerve (cranial nerve X) is the longest nerve of the autonomic neuronal system. It is a mixed nerve, consisting of ~80% sensory fibres carrying information from the body to the brain. These sensory fibres project mainly to the nucleus of the solitary tract (Van Bockstaele et al., 1999). This nucleus, in turn, projects to the pontine region, cerebellum, mesencephalon and amygdala. Furthermore, there is anatomical evidence demonstrating that the vagal nerve projects directly to the dorsal raphe nucleus and indirectly to the locus coeruleus (Dorr and Debonnel, 2006; Bland et al., 2016). Interestingly, both the above-mentioned structures send direct projections to the hippocampal formation (HPC), which is engaged in the generation of epileptiform discharges in temporal lobe epilepsy (Castle et al., 2005). The HPC is also considered to be the main structure involved in the generation of the theta rhythm. This type of regular electroencephalographic (EEG) activity is the most spectacular example of oscillations and synchrony which appear in the mammalian brain (Bland, 1986; Bland and Colom, 1993; Buzsáki, 2002). On the basis of behavioral correlates and drug manipulation, two types of the hippocampal theta rhythms were distinguished in rats. One is labelled type 1 and the second type 2

* Corresponding author at: Department of Neurobiology, Faculty of Biology and Environmental Protection, The University of Lodz, Pomorska Str. No 141/143, 90 – 236 Łódź, Poland.
E-mail addresses: adam.broncel@neuromedical.pl (A. Broncel), renata.bocian@biol.uni.lodz.pl (R. Bocian), paulina.klos@biol.uni.lodz.pl (P. Kłos-Wojtczak), jan.konopacki@biol.uni.lodz.pl (J. Konopacki).

https://doi.org/10.1016/j.brainresbull.2018.05.005
Received 1 March 2018; Received in revised form 25 April 2018; Accepted 4 May 2018
Available online 06 May 2018
0361-9230/

(Vanderwolf, 1969; Kramis et al., 1975; Bland, 1986). Type 1 theta (7–12 Hz) occurs while walking, running, swimming and other voluntary behaviors (Vanderwolf, 1969; Bland, 1986; Sainsbury and Partlo, 1993). This type of theta is relatively unaffected by large doses of atropine sulphate but is abolished by ethyl ether and urethane (Kramis et al., 1975; Bland, 1986). Type 2 theta (3–6 Hz) has occasionally been recorded during immobility, licking, chewing and other automatic activities (Bland, 1986; Sainsbury, 1985). This type of theta is induced by cholinergic (muscarinic) agonists and can be abolished by an injection of atropine sulphate, and is resistant to most anesthetics (Bland and Colom, 1993; Sainsbury, 1985).

Numerous studies indicate that the theta rhythm is involved in long-term potentiation (LTP; Huerta and Lisman, 1995; Natsume and Kometani, 1997), spatial learning and navigation (Mehta, 2015; Pu et al., 2017), locomotor activities (Oddie and Bland, 1998), sensory-motor integration (Bland and Oddie, 2001), working memory (Mesbah-Oskui et al., 2015), and REM sleep (Bódizs et al., 2001). The involvement of theta-band oscillatory mechanisms in LTP, locomotor activities, sensory-motor integration and pathological neuronal discharges suggests that analyzing the mechanisms of theta field potentials could yield important information concerning memory processing, movement selection, as well as the etiology of epilepsy or Alzheimer's disease (Hyman et al., 1984; Colom, 2006; Chauviere et al., 2009; Adaya-Villanueva et al., 2010).

The first data showing the effect of VNS on hippocampal EEG activity comes from Larsen's studies (Larsen et al., 2016a,b). These authors demonstrated that VNS modulated the evoked potentials, reduced total power of the hippocampal EEG, and slowed the theta rhythm in freely-moving rats. However, recently, Broncel et al. (2017) have obtained quite different results in anesthetized rats. Specifically, these authors reported that the effect of VNS on the HPC theta rhythm in the anesthetized rats depends on the applied protocol and the current intensity. In urethanized rats VNS could induce theta activity during stimulation when high intensity VNS is applied or, with some delay, when lower intensity stimuli were used (a direct and delayed effect, respectively).

The fact that the HPC theta rhythm can be produced, depending on current intensity, directly during VNS or after this procedure suggests that this EEG pattern can also be used as a bio-indicator of the efficiency of VNS. In the present study, we focused on three specific technical issues related to the stimulation procedure of the vagal nerve: i/does the type of electrode used for VNS and the technique of its implantation affect the parameters of the HPC theta rhythm? ii/does the type of electrode used determine the current intensity threshold of VNS-induced HPC theta? iii/is the repeatability of the VNS effect determined by the type of electrode used?

2. Materials and method

All experiments described below were monitored by the Local Ethical Commission (permissions no. 5/LB13/2016 in accordance with the European Communities Council Directive of November 24, 1986).

2.1. Subjects and surgical procedure

The data were obtained from 59 male Wistar rats (160–200 g) housed on a 12 h light/dark cycle with free access to water and food. The rats were initially anesthetized with isoflurane (Baxter, Belgium) while a jugular cannula was inserted. Isoflurane was then discontinued, and urethane (0.6 g/ml, Sigma Chemical Co., USA) was administered via the jugular cannula in order to maintain anesthesia throughout the experiment. The anesthesia level was maintained so that theta field potentials and the transition from theta to irregular activity could occur spontaneously. Body temperature was maintained at 36.5 °C ± 0.5 °C by a heating pad and heart rate was monitored constantly throughout the experiment.

In the next step of the surgery, the left vagal nerve was isolated from the carotid artery using glass section sticks. The left branch of the vagal nerve was chosen to minimize negative cardiac effect (e.g. bradycardia or asystole) observed during electrical stimulation (Howland, 2014). Then the animals were placed in a stereotaxic frame with the plane between the bregma and lambda levelled to horizontal. An uninsulated tungsten wire, placed in the cortex 2 mm anterior to the bregma, served as an indifferent electrode, and the stereotaxic frame was connected to the ground. A tungsten microelectrode (0.3–0.9 MΩ) for recording hippocampal field activity was placed in the right dorsal HPC, in the stratum lacunosum-moleculare (3.2 mm posterior from the bregma, 2.0–2.2 mm lateral from the midline, and 2.6–2.8 mm ventral to the dural surface; Paxinos and Watson, 2014). An AC amplifier (P-511, Grass-Astromed, USA) was used for recording the field potentials, with the low-filter set at 1 Hz and the high-filter set at 0.3 kHz. The field activity was displayed using a digital storage oscilloscope (Tektronix –TDS 3014B, Beaverton, USA). The EEG signals were digitalized with the interface (1410 plus, Cambridge Electronic Design, GB) and recorded onto a computer hard disk for subsequent off-line analysis (Spike 2.29, Cambridge Electronic Design, GB).

2.1.1. Experiment 1

Experiment 1 examined whether the implanted vagal cuff electrode affects the HPC theta parameters. In the present study, the theta epoch was recognized as rhythmic, high amplitude, sinusoidal waveforms in a strictly defined frequency i.e. 3–6 Hz.

2.1.1.1. Experimental procedures. Fifteen animals were divided into three groups (Table 1). Group 1: In the animals of the first group the recording electrode was implanted unilaterally into the HPC to register the local spontaneous field activity. Group 2: In the animals of the second group, at the beginning of the surgical procedure the vagal nerve was isolated, moisturized with glycerine (Aflofarm, Poland) and marked by two threads. Next, the recording electrode was implanted into the HPC for registration of local field potentials. Group 3: In the animals of the third group, before implantation of the HPC recording electrode, the vagal nerve was isolated, moisturized with glycerine (Aflofarm, Poland) and a platinum-iridium cuff stimulating electrode was implanted. The cuff electrode surrounded the vagal nerve and had contact with it throughout the entire experiment. During experiment 1 the spontaneous hippocampal EEG activity was registered in each rat for 30 min. Please note that in experiment 1 VNS was not applied.

2.1.1.2. Data analysis. The EEG data obtained from experiment 1 were analyzed off-line using the Spike-2.29 software computing system. Ten 3-s epochs of spontaneous hippocampal theta recorded in each animal of the first group were subjected to power/frequency (FFT) analysis. FFT size was 128 (0.03072 s), window honning, frequency from 0 to 50 Hz in 64 bins, resolution 0.7813 Hz. The mean peak-to-peak amplitude of theta was determined directly from the epochs of theta. The same procedure of analysis was precisely repeated for the data of the second and the third groups.

2.1.1.3. Statistical analysis. Two measured parameters (amplitude and frequency) of the spontaneous theta activity were subjected to the Shapiro-Wilk test to check normal distribution of the data. Then, a Mann-Whitney *U* test was performed (Statistica 12, StatSoft, Poland). For amplitude and frequency the mean ± SE was calculated.

2.1.2. Experiment 2

Experiment 2 consisted of two stages. The first stage of this experiment was focused on the examination of whether the type of the electrode used determines the current intensity threshold of VNS-induced the hippocampal theta rhythm. The second stage was designed to answer the question of whether the type of electrode used determines the repeatability of the VNS effect on HPC field potential.

Table 1
The characteristics of the experimental groups used in Experiment 1 and Experiment 2.

EXPERIMENT 1:		
GROUP 1	GROUP 2	GROUP 3
Animals with: - implanted recording electrode into HPC (n = 5)	Animals with: - isolated and marked vagal nerve, - implanted recording electrode into HPC (n = 5)	Animals with: - isolated vagal nerve and implanted cuff electrode, - implanted recording electrode into HPC (n = 5)

EXPERIMENT 2:			
GROUP 1		GROUP 2	
Animals with: - isolated and marked vagal nerve, - implanted recording electrode into HPC		Animals with: - isolated vagal nerve and implanted cuff electrode, - implanted recording electrode into HPC	
VNS provided with use of tungsten fork electrode		VNS provided with use of platinum-iridium cuff electrode	
number of subgroup	parameters of VNS/ number of animals (n)	number of subgroup	parameters of VNS/ number of animals (n)
I	1 mA, 1 ms, 10 Hz (n = 4)	I	1 mA, 1 ms, 10 Hz (n = 4)
II	2 mA, 1 ms, 10 Hz (n = 4)	II	2 mA, 1 ms, 10 Hz (n = 4)
III	4 mA, 1 ms, 10 Hz (n = 4)	III	4 mA, 1 ms, 10 Hz (n = 4)
IV	6 mA, 1 ms, 10 Hz (n = 4)	IV	6 mA, 1 ms, 10 Hz (n = 4)
V	8 mA, 1 ms, 10 Hz (n = 4)	V	8 mA, 1 ms, 10 Hz (n = 4)
VI	10 mA, 1 ms, 10 Hz (n = 4)		

n – number of animals. mA – stimulus intensity; ms – pulse duration; Hz – frequency.

2.1.2.1. Stage 1: experimental procedures. Forty four animals were divided into two groups (Table 1). Group 1: In the first group of animals (n = 24) the vagal nerve was isolated, moisturized with glycerine (Aflofarm, Poland) and marked by two threads. Next, the recording electrode was implanted into the HPC. After the implantation of the HPC recording electrode, the animals were left for 30–45 min to adapt to the experimental conditions. VNS was applied with the use of a handmade tungsten bipolar fork electrode (0.1–0.2 kΩ Fig. 1). Based on the different current intensity used for VNS, six subgroups were extracted (Table 1). In the first subgroup current pulse intensity was 1 mA, and in subgroups from two to six 2, 4, 6, 8 and 10 mA, respectively. The other VNS parameters were constant in all the subgroups: pulse duration 1 ms, train duration 10 s, frequency 10 Hz. Constant current square pulses were delivered through an isolation unit (PSIU6, Grass-Astromed, West Warwick, USA) from the stimulator (S48 Grass-Astromed, West Warwick, USA). In the animals of this group the tungsten bipolar fork stimulating electrode touched the vagal nerve surface only during stimulation.

Group 2: In the second group of animals (n = 20), before the implantation of the recording electrode into the HPC, a commercially available platinum-iridium cuff stimulating electrode (40 kΩ; SPM35 10 HY, MicroProbe, USA; Fig. 1) was implanted on the vagal nerve. Before implantation of the cuff electrode, the vagal nerve was moisturized with glycerine (Aflofarm, Poland). Based on the different current intensity used for VNS, five subgroups were extracted (Table 1). In the first subgroup current pulse intensity was 1 mA, and in subgroups from two to five 2, 4, 6 and 8 mA, respectively. The other VNS parameters were constant in all the subgroups: pulse duration 1 ms, train duration 10 s, frequency 10 Hz. The square pulse was delivered through an isolation unit (PSIU6, Grass-Astromed, West Warwick, USA) from the stimulator (S48, Grass-Astromed, West Warwick, USA). In animals of this group the cuff stimulating electrode surrounded the nerve and had contact with it throughout the entire experiment.

During the first stage of experiment 2, in both experimental groups, the stimulation of the vagal nerve was always applied at a moment when no spontaneous theta was present in the hippocampal field potential.

2.1.2.2. Stage 2: experimental procedures. Four animals from subgroup VI of group 1 and four from subgroup V of group 2 were also utilized in the second step of experiment 2. After a 15-min interval, the rats from both above-mentioned subgroups were subjected to a second stimulation of the vagal nerve (VNS-2) using exactly the same parameters as during the first stimulation (VNS-1). The second VNS was also applied at a moment when no spontaneous theta was present in hippocampal field potential.

2.1.2.3. Statistical analysis. The amplitude and frequency of the VNS-induced theta recorded were subjected to the Wilcoxon matched-pairs signed-rank test (Statistica 12, StatSoft, Poland). For amplitude and frequency a mean ± SE was calculated.

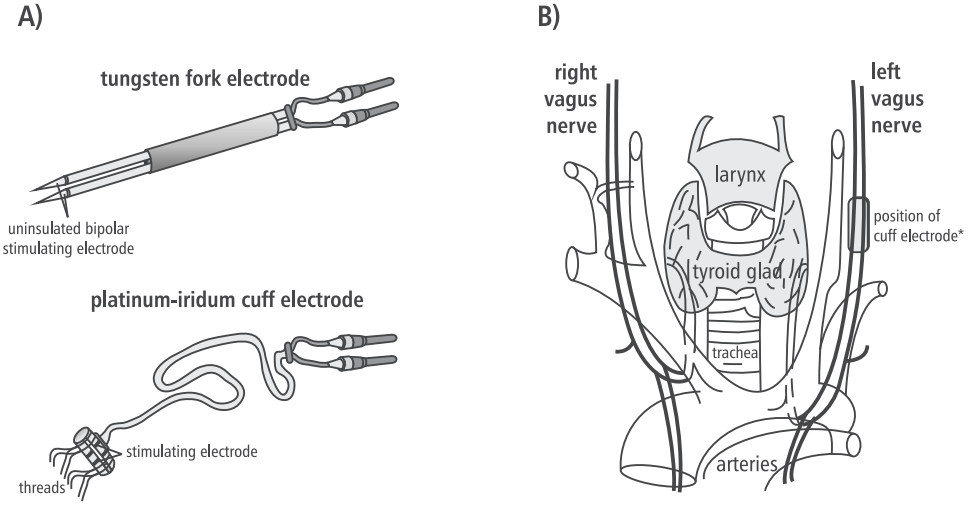

Fig. 1. Diagrammatic representation of the vagal nerve stimulation arrangement. A/ Scheme of the tungsten bipolar fork electrode and platinum-iridium cuff electrode. B/ Illustration of the vagal nerve course, with the position of the cuff stimulating electrode marked. *Please note: the position of the fork electrode was similar.

2.2. Histological procedure

In all the animals the recording electrode tip location was marked by passing a 15 μA current for 14 min (7 min cathodal, 7 min anodal, S48 stimulator; Grass-Astromed, West Warwick, USA). Next, the rats were sacrificed by an overdose of urethane for histological examination. The brains were removed and stored in 10% formalin. Frozen brain sections (30 μm) were taken serially and mounted on glass slides for the reconstruction of HPC theta recording sites.

3. Results

Histological analysis revealed that in all the rats the electrodes for recording dorsal HPC theta activity were located in the region of the stratum lacunosum-moleculare between the frontal planes, 3.0-3.2 mm posterior from the bregma (Paxinos and Watson, 2014), data not shown.

3.1. Experiment 1

Group 1: In all animals from group 1 the spontaneous theta rhythm was never observed to occur continuously. Typically, the irregular field activity recorded from the HPC of anesthetized rats was separated by trains of theta epochs (Fig. 2, upper row, left side). The power/frequency spectrographs of the representative analogue samples of hippocampal spontaneous theta field activity recorded in animals from group 1 is shown in Fig. 2A (upper row, right side). Detailed analysis of the spontaneous theta rhythm parameters recorded in rats in this group revealed that the mean values of amplitude and frequency were as follows: 524.65 ± 51.68 μV and 4.67 ± 0.2 Hz (Fig. 2B).

Group 2: In the animals of group 2 (i.e. with isolated and marked vagal nerves) the spontaneous theta rhythm was also never observed to occur continuously. In the hippocampal EEG trains of theta, epochs were separated by irregular activity (Fig. 2, middle row, left side). The power/frequency spectrographs of representative analogue samples of hippocampal spontaneous theta field activity recorded in animals from group 2 is shown in Fig. 2A (middle row, right side). The amplitude and frequency of the theta rhythm recorded in rats from group 2 were close to the amplitude and frequency observed in animals from group 1 (567.65 ± 86.34 μV and 4.55 ± 0.1 Hz; Fig. 2B).

Group 3: The rats from group 3 (i.e. with isolated vagal nerve and implanted cuff electrode), similar to animals from group 1 and 2, produced regular activity in the theta band in short epochs (Fig. 2A, the lowest row, left side). The power/frequency spectrographs of representative analogue samples of hippocampal spontaneous theta field activity recorded in rats from group 3 is shown in Fig. 2A (the lowest row, right side). Detailed analysis revealed that the theta amplitude recorded in animals from group 3 were significantly lower in comparison with the same parameter recorded in rats from both group 1 (417.32 ± 49.98 μV vs 524.65 ± 51.68 μV, $p < 0.01$) and group 2 (417.32 ± 51.98 μV vs 567.65 ± 86.34 μV, $p < 0.01$; Fig. 2A and Fig. 2B). In contrast to the amplitude, the mean value of theta frequency (4.49 ± 0.2 Hz) recorded in rats from group 3 was comparable to the value observed in animals from group 1 and group 2 (Fig. 2B).

3.2. Experiment 2

3.2.1. Stage 1

The effect of single VNS applied with the use of a tungsten fork (group 1) or platinum-iridium cuff electrodes (group 2) on hippocampal EEG activity is shown in Fig. 3. In animals in group 1 the VNS intensity applied in the range of 1–8 mA did not induce any apparent effect on the HPC field potential during stimulation (VNS-1, Fig. 3A and B upper and middle left panel). The threshold intensity of VNS capable of inducing the HPC theta rhythm in the anesthetized rats was 10 mA (Fig. 3A). This effect is visible in the analogue example of HPC field potential and the related FFT histogram (Fig. 3B, the lowest left panel).

In animals in group 2 VNS intensity applied in the range of 1–6 mA did not induce any apparent effect on the HPC field potential during stimulation (Fig. 3A and B upper right panel). The VNS threshold intensity capable of inducing the theta rhythm was 8 mA (Fig. 3A and B lower right panel). The effect of VNS in 8 mA intensity is visible in the analogue example of HPC field potential and the related FFT histogram (Fig. 3B, lower right panel).

3.2.2. Stage 2

The effect of the second vagal nerve stimulation (VNS-2), carried out using the same parameters as VNS-1 on hippocampal EEG activity, is shown in Fig. 4. In the animals in subgroup VI of group 1, VNS-2 applied in threshold intensity of 10 mA failed to induce theta activity (Fig. 4A, upper right row). In the animals in subgroup V of group 2, VNS-2 applied in threshold intensity of 8 mA produced well-synchronized theta (Fig. 4A, lower right row).

Statistical analysis revealed that the amplitude of VNS-induced the hippocampal theta rhythm recorded during VNS-1 in rats in subgroup VI of group 1 was higher in comparison to VNS-induced theta registered in animals in subgroup V of group 2 (573.24 ± 51.67 μV vs 439.75 ± 48.11 μV, $p < 0.05$). In contrast to the amplitude, the mean values of VNS-induced theta frequency recorded in rats of both subgroups were similar (4.61 ± 0.2 Hz; 4.43 ± 0.1 Hz; Fig. 4B), while in the VNS-2 induced theta rhythm (subgroup V of group 2), the parameters of recorded rhythmic slow activity were comparable to the parameters of theta observed during the first stimulation (Fig. 4B).

4. Discussion

Vagal nerve stimulation (VNS) therapy has become a prominent fixture in treatment research and has been proposed as a therapy for many neurological and neuropsychiatric disorders (Ben-Menachem, 2002; Mauskop, 2005; Merrill et al., 2006; Aalbers et al., 2011; Howland et al., 2011; Howland, 2014; Xiang et al., 2015; Hays et al., 2016; Neren et al., 2016). While VNS was approved for seizure prevention in epilepsy and as an alternative for many other neural disorders, the exact mechanisms of much of the body's response to VNS has yet to be characterized. An abundance of clinical studies demonstrates a 50% reduction in seizure frequency in about 1/3 of patients with refractory epilepsy resulting from diverse clinical conditions (Ben-Menachem, 2002; Boon et al., 2002). This is still not a satisfactory percentage for the efficiency of this therapy. Unfortunately, up to now, there have not been precisely-identified factors that could explain the relatively low VNS efficiency. Technical issues connected with electrode implantation and nerve stimulation could be crucial for the final effect of VNS.

There are many aspects which ought to be considered when approaching VNS in animal experiments. The first major issue is whether to attempt a chronic or acute study. The long-term effects of VNS treatment over days, weeks, and even years cannot be accurately studied acutely. Moreover, due to the nature of the anesthetic used in acute surgical procedure, potential unintended and detrimental physiological effects on the body's normal state can be caused. As it was demonstrated by Picq et al. (2013), the immunoregulatory effects of isoflurane can influence the results of studies conducted with the use of VNS. The second important aspect of VNS is the established protocol which determines the stimulation parameters and stimulation intervals. The great variability of VNS protocols have been widely discussed previously (Aalbers et al., 2011). In the present study, we raised one more important aspect of VNS. For optimizing VNS effects, it is mandatory to realize the side effects of the electrode *per se*. Specifically, we focused on the evaluation of the specific physiological effect of two different stimulation electrodes: tungsten fork bipolar electrodes, rarely utilized in experimental conditions (Broncel et al., 2017), and cuff platinum-iridium bipolar electrodes. The model of the HPC type II theta

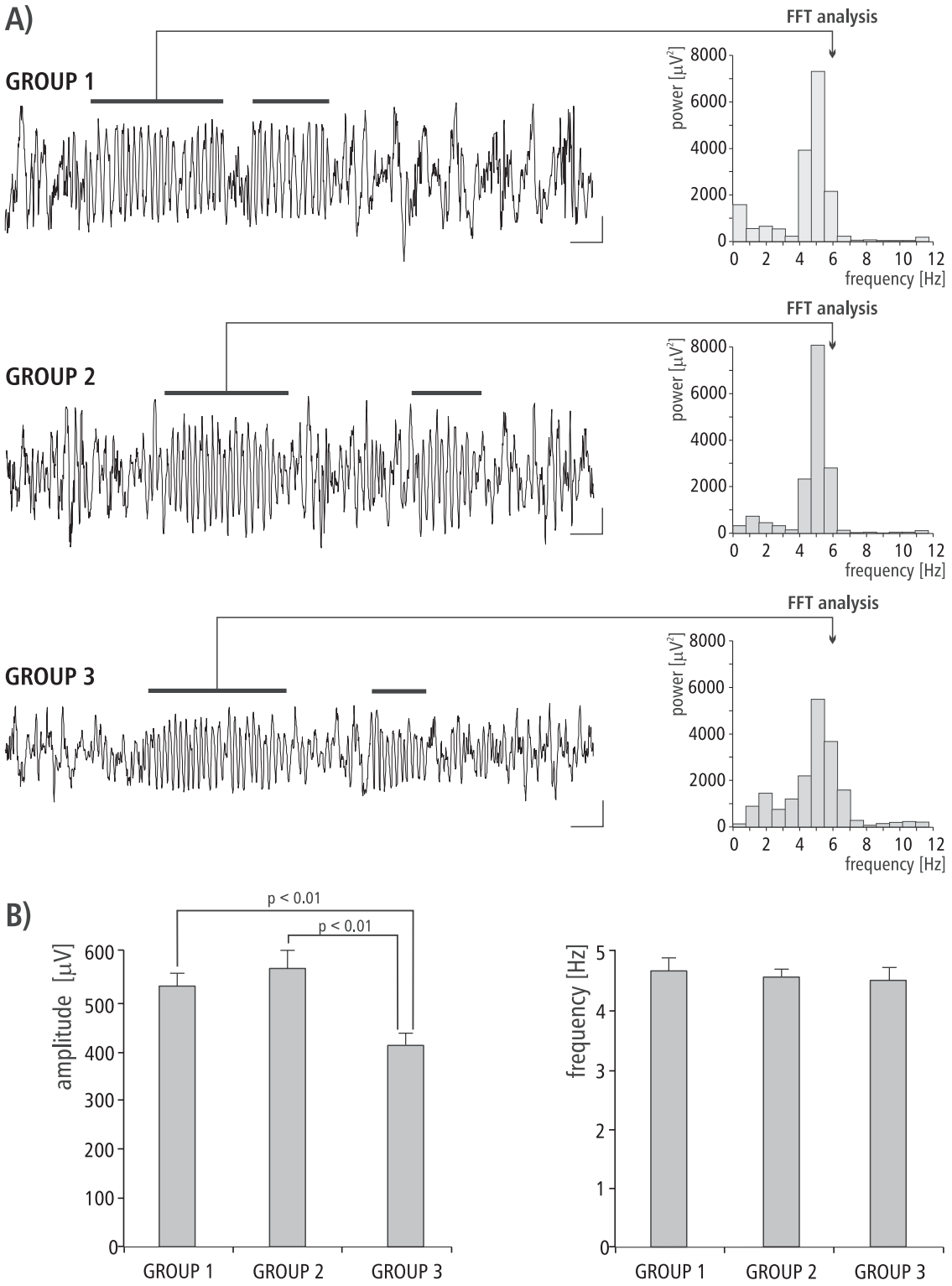

Fig. 2. The effect of platinum-iridium cuff electrode implantation on the spontaneous hippocampal theta rhythm. A/The spontaneous EEG activity recorded from the hippocampal formation and related power-frequency (FFT) histogram registered in animals from groups 1, 2 and 3. The spontaneous theta activity was marked with a black horizontal line. B/Mean values (± SE) of amplitude and frequency of the spontaneous theta activity recorded in animals from groups 1, 2 and 3. Statistical analysis: Mann-Whitney *U* test. Calibration: 200 μV, 1s.

rhythm was employed as a biomarker for testing the physiological effect of the electrodes themselves and the efficacy of VNS.

4.1. Experiment 1

The first experiment was specifically designed to evaluate the effect of the vagal cuff electrode *per se* on the HPC theta rhythm. We demonstrated that the implanted cuff platinum-iridium electrode significantly decreased the amplitude of HPC theta. The cuff electrode can cause some morphological changes in the vagal nerve, whose influences in the final host response may often overlap. Analyzing the possible mechanisms of this effect, at least five basic factors should be

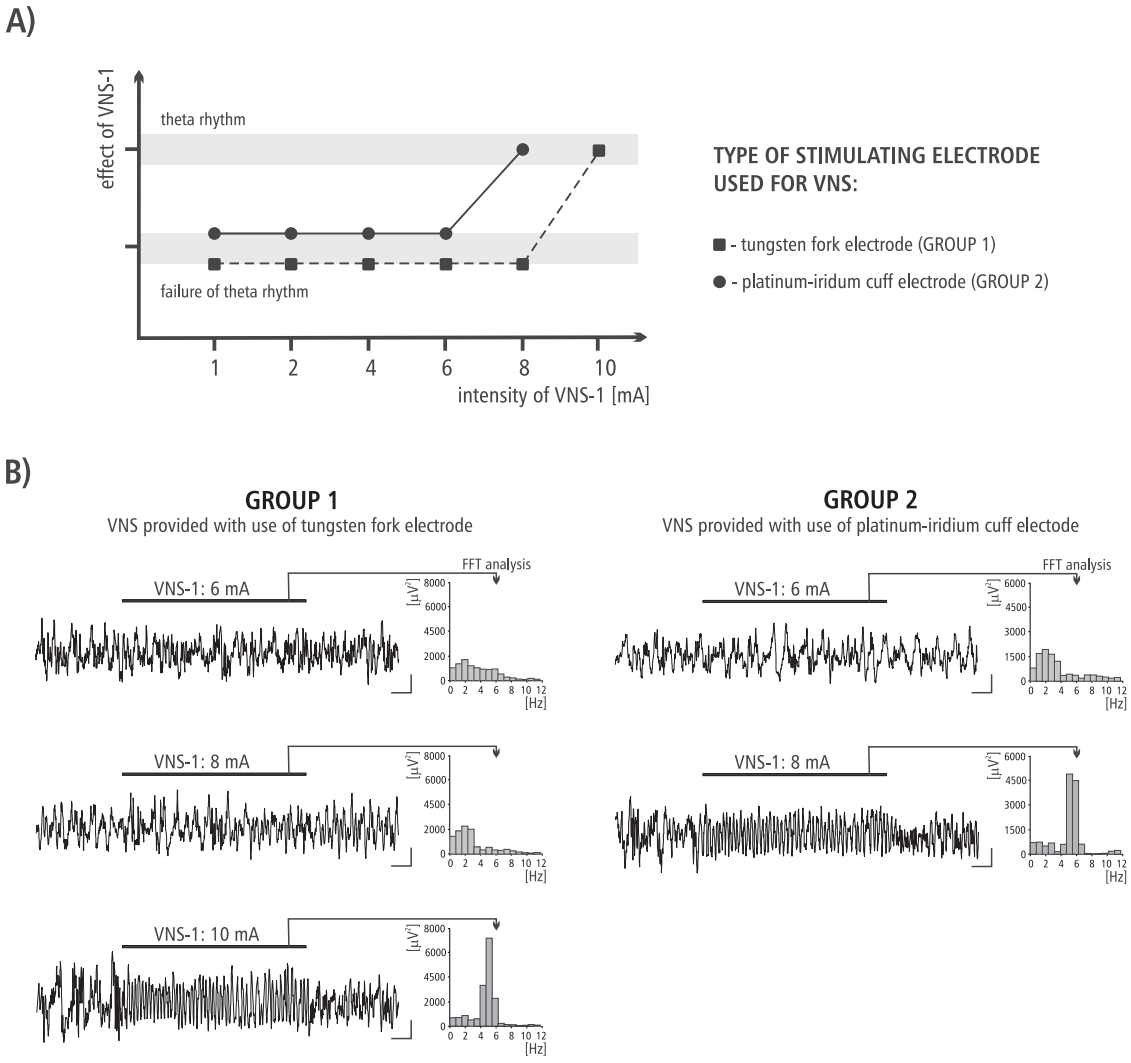

Fig. 3. Direct effect of single vagal nerve stimulation (VNS-1) provided with the use of two different types of electrode on hippocampal EEG activity. A/The current intensity threshold of VNS-induced hippocampal theta rhythm recorded in animals of group 1 and group 2. The range of VNS was 1–10 mA. B/Representative analogue samples of hippocampal EEG activity recorded during VNS-1 in ranges 6, 8 and 10 mA and the related power-frequency (FFT) histogram in animals in group 1 (left panel) and group 2 (right panel, VNS-1 in ranges 6–8 mA). Time of VNS-1 was marked with a black horizontal line. Calibration: 200 μV, 1s.

considered: 1/the surgical manipulation of the vagal nerve during the implantation procedure, 2/the inflammatory reaction, 3/the electrochemical processes, 4/the mechanical irritation of the vagal nerve induced by the plastic cuff and 5/cuff compression on the vagal nerve. Although all the above-mentioned factors can induce an immediate or long-term structural reaction of the nerve, in the case of the above-described experiments, only a brief effect existed, since the time interval between the cuff electrode implantation and HPC theta recording was no more than 2 h. Hence, the inflammatory effect can be probably omitted, since it requires a longer time for development and detection (Yuen et al., 1984; Díaz-Güemes Martín-Portugués et al., 2005).

It is also possible that damage to the vagal nerve is due in part to the electrochemical processes at the electrode/tissue interface (McCreery et al., 1992). These processes depend on pulse duration, current intensity, pulse frequency, the total time of stimulation and the quality of the electrode used (Agnew et al., 1989; Rose and Robblee, 1990). All current parameters were identical both for tungsten and platinum iridium electrodes. However, the electrode/tissue interface exposition was different – about 2 h for the cuff electrode and 10 s for the tungsten electrode. Hence, we cannot discuss and to compare this issue in detail.

Short and light mechanical irritation of the vagal nerve induced by micro-movements of the plastic cuff induces rather short excitation of the vagal nerve. However, even in the anesthetized rats which remain practically still in the stereotactic frame, micro-movements of the cuff can be induced even by the respiratory activity of the chest. This effect probably overlaps the influence of the cuff compression (Vanhoestenberghe, 2013). The cuff compression neuropathy may result from the far smaller inner diameter of the cuff (Díaz-Güemes Martín-Portugués et al., 2005; Ordonez et al., 2014). The cuff electrodes used in our experiments were specifically designed and manufactured for the vagal nerve in rats. However, the cuff electrodes require sutures to close the cuff's opening split and to hold the electrode in place, making an additional compression level that is difficult to control. This compression may result in uncontrolled nerve damage. It was previously demonstrated that graded compression of a peripheral nerve quickly induced inhibition of the axonal transport (Dahlin et al., 1984) as a possible result of axonal damage (Ochoa et al., 1972). We did not quantify morphological disturbances of the vagal nerve in the present study. However, the impact of these structural changes on nerve activity was previously described in sensory nerves by Slot et al. (1997). These authors demonstrated the initial decline of the action potential amplitude and recovery after 10 days. In our experiments the only notable symptom of the cuff electrode implantation itself was the apparent 25% decrease in amplitude and power of the HPC theta rhythm.

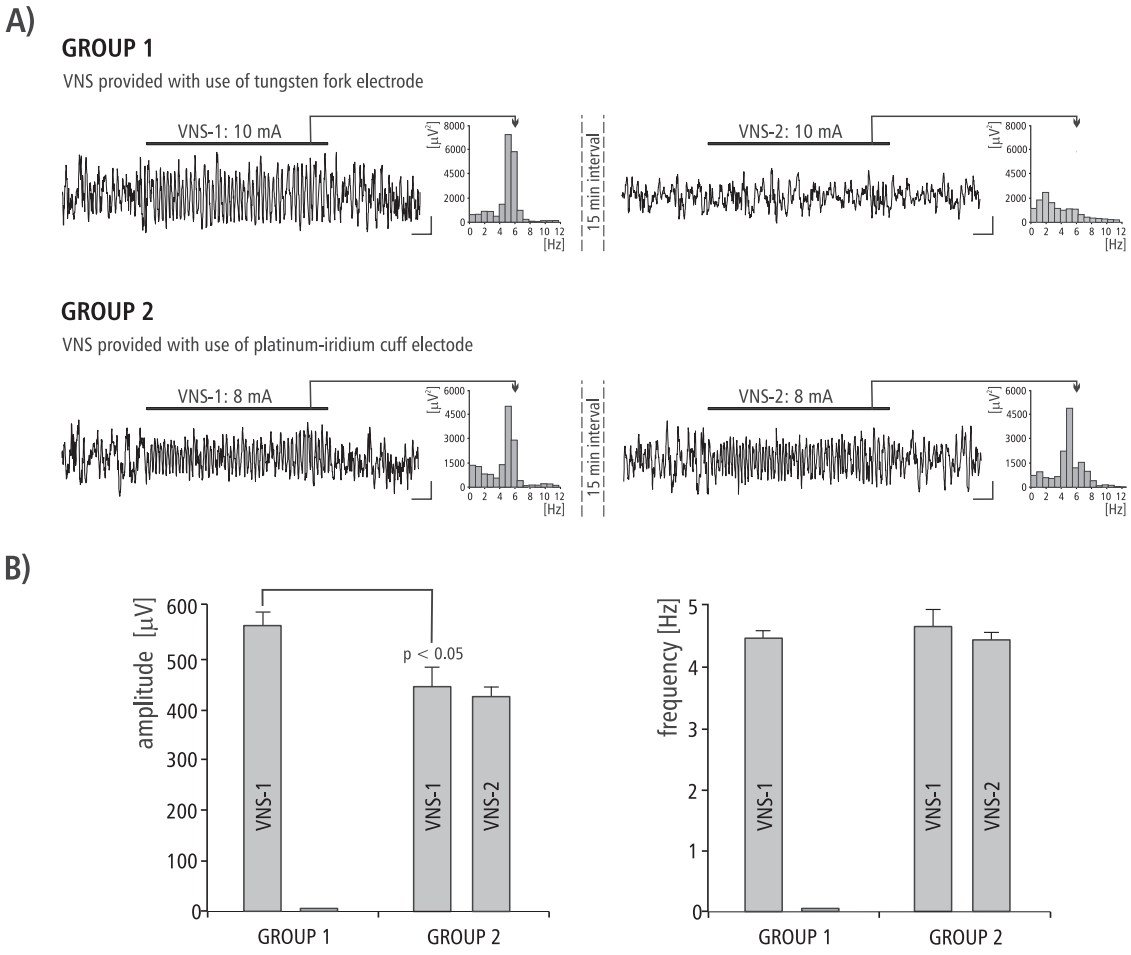

Fig. 4. The effect of double VNS stimulation on hippocampal EEG activity. A/Representative analogue samples of hippocampal EEG activity recorded during the first and the second vagal nerve stimulation (VNS-1 and VNS-2, respectively) and the related power-frequency (FFT) histogram in animals in group 1 (subgroup VI) and group 2 (subgroup V). Time of VNS was marked with a black horizontal line. Calibration: 200 μV, 1s. B/Mean values (± SE) of amplitude and frequency of VNS-induced theta activity recorded during VNS-1 and VNS-2 in animals in group 1 (subgroup VI) and group 2 (subgroup V). Statistical analysis: Wilcoxon matched-pairs signed-rank test.

This is definitively a secondary effect, since HPC does not receive the vagal afferents directly. The question arises as to the possible mechanism of HPC theta amplitude decrease. This mechanism probably goes beyond the vagal nerve itself. The induction of type II theta rhythm in the HPC depends on the activation of a number of structures: from the pontine region, via the hypothalamus, up to the basal parts of the forebrain, which form the ascending brainstem hippocampal synchronizing pathway (Oddie et al., 1994; Vertes and Kocsis, 1997; Bland and Oddie, 1998; Bland, 2000). The medial septum is considered to be a nodal point of this pathway, since rhythmic outputs from the medial septum area act as a "pacemaker" for the HPC theta rhythm (Monmaur and Breton, 1991; Bland and Colom, 1993; Lee et al., 1994; Vertes and Kocsis, 1997; Bland, 2000; Kang et al., 2015). The medial septum integrates not only central inputs from the brainstem synchronizing pathway but also input from the NST, the primary relay site of vagal afferents in the brain stem (Castle et al., 2005). In the light of the above-mentioned data, the decreased axonal transport in the vagal nerve in response to vagal compression and the mechanical micro-irritation may result in decreased vagal input to NST and, further, the decreased NST input to the medial septum which determines the amplitude of the HPC theta rhythm. This hypothesis would support an earlier suggestion concerning vagal multisynaptic relays to the HPC (Castle et al., 2005). Additionally, the cuff electrode micro-irritation could activate ascending inhibitory inputs to hippocampus, for example, via the raphe nucleus, to depress theta (Bland et al., 2016).

4.2. Experiment 2

Experiment II examined whether the type of the electrode used determines the current intensity threshold of VNS-induced the HPC theta rhythm (stage 1) and its repeatability (stage 2). It was demonstrated that in comparison with tungsten fork bipolar electrodes the use of platinum-iridium bipolar cuff electrode decreases the intensity threshold of VNS necessary to produce the HPC theta rhythm. In addition, the repeatability of the VNS effect on HPC theta field potential was observed only when the cuff electrode was used. This result was unexpected. In contrast to the platinum-iridium cuff electrode, the tungsten electrode touched the vagal nerve only during the stimulation. This strategy was employed to avoid or eliminate or decrease potential histopathological changes associated with the mechanical irritation of the vagal nerve induced by the cuff (Agnew and McCreery, 1990; Díaz-Güemes Martín-Portugués et al., 2005). Interestingly, the second VNS applied with use of tungsten electrode failed to produce pronounced rhythmic field activity. This result is not surprising if we consider the fact that the current intensity of 10.0 mA is rather high and could induce vagal damage by fibre hyperexcitation (Agnew et al., 1990; Rodríguez et al., 2000; Díaz-Güemes Martín-Portugués et al., 2005). If this was the case, it would result in the abolishment of the brief effect of the second VNS on HPC field potential. An alternative mechanism for the decrease efficacy of the tungsten electrode for second response tests could be that tungsten is known to polarize more than platinum-iridium

and this polarization would increase the resistance at the tips of the stimulating electrode and so would decrease the current/voltage of stimulation (Geddes and Roeder, 2003; Stevenson et al., 2010).

Finally, one more issue to be addressed in the present study was the VNS provided in rats in which the level of anesthesia was strictly maintained at a constant level during the entire experiment, i.e. such that theta field potentials and the transition from theta to irregular activity could occur spontaneously. Interestingly, in the previous experiments the anesthesia prevented axonal degeneration (Agnew et al., 1990) and modulated the effects of VNS, because non-anesthetized animals needed higher intensity current pulses of VNS than anesthetized animal to obtain anticonvulsive effect (Woodbury and Woodbury, 1990; Aalbers et al., 2011). This would indicate that the level of arousal is also an essential factor that determines the final host effect of VNS.

In conclusion, we have compared the vagal effect of the platinum-iridium cuff electrode and the tungsten fork electrodes on HPC field potential. We demonstrated that the platinum-iridium cuff electrode offers some important advantages that the tungsten electrode does not. Firstly, despite some possible mechanical and compression nerve damage related to permanent contact with the vagal nerve, it offers a lower current intensity threshold for inducing theta oscillations in the limbic cortex. Secondly, and most importantly, is that the cuff electrode offers the repeatability of the VNS effect on HPC theta field potential. However, one disadvantage of using this type of electrode for the VNS effect on EEG is that permanent pressure of the vagal nerve by the cuff itself may decrease the amplitude of the investigated field potential.

Conflict of interest

The authors declare that there are no conflicts of interest.

Acknowledgements

This work was supported by grant from Regional Operational Programme for Lodzkie Voivodeship for 2014–2020 (grant number: RPLD.01.02.02-10-0067/17-00).

References

Aalbers, M., Vles, J., Klinkenberg, S., Hoogland, G., Majoie, M., Rijkers, K., 2011. Animal models for vagus nerve stimulation in epilepsy. Exp. Neurol. 230, 167–175.
Adaya-Villanueva, A., Ordaz, B., Balleza-Tapia, H., Márquez-Ramos, A., Peña-Ortega, F., 2010. Beta-like hippocampal network activity is differentially affected by amyloid beta peptides. Peptides 31, 1761–1766.
Agnew, W.F., McCreery, D.B., 1990. Considerations for safety with chronically implanted nerve electrodes. Epilepsia 31 (Suppl. 2), S27–32.
Agnew, W.F., McCreery, D.B., Yuen, T.G., Bullara, L.A., 1989. Histologic and physiologic evaluation of electrically stimulated peripheral nerve: considerations for the selection of parameters. Ann. Biomed. Eng. 17, 39–60.
Agnew, W.F., McCreery, D.B., Yuen, T.G., Bullara, L.A., 1990. Local anaesthetic block protects against electrically-induced damage in peripheral nerve. J. Biomed. Eng. 12, 301–308.
Bódizs, R., Kántor, S., Szabó, G., SzÛcs, A., Erõss, L., Halász, P., 2001. Rhythmic hippocampal slow oscillation characterizes REM sleep in humans. Hippocampus 11, 747–753.
Ben-Menachem, E., 2002. Vagus-nerve stimulation for the treatment of epilepsy. Lancet Neurol. 1, 477–482.
Bland, B.H., Colom, L.V., 1993. Extrinsic and intrinsic properties underlying oscillation and synchrony in limbic cortex. Prog. Neurobiol. 41, 157–208.
Bland, B.H., Oddie, S.D., 1998. Anatomical, electrophysiological and pharmacological studies of ascending brainstem hippocampal synchronizing pathways. Neurosci. Biobehav. Rev. 22, 259–273.
Bland, B.H., Oddie, S.D., 2001. Theta band oscillation and synchrony in the hippocampal formation and associated structures: the case for its role in sensorimotor integration. Behav. Brain Res. 127, 119–136.
Bland, B.H., Bland, C.E., MacIver, M.B., 2016. Median raphe stimulation-induced motor inhibition concurrent with suppression of type 1 and type 2 hippocampal theta. Hippocampus 26, 289–300.
Bland, B.H., 1986. The physiology and pharmacology of hippocampal formation theta rhythms. Prog. Neurobiol. 26, 1–54.
Bland, B.H., 2000. The medial septum: node of the ascending brainstem hippocampal synchronizing pathways. In: Numan, R. (Ed.), The Behavioral Neuroscience of the Septal Region. Springer-Verlag, New York, pp. 115–145.
Boon, P., Vonck, K., de Reuck, J., Caemaert, J., 2002. Vagus nerve stimulation for refractory epilepsy. Seizure 11, 448–455.
Broncel, A., Bocian, R., Kłos-Wojtczak, P., Konopacki, J., 2017. Vagus nerve stimulation produces a hippocampal formation theta rhythm in anesthetized rats. Brain Res. 1675, 41–50.
Buzsáki, G., 2002. Theta oscillations in the hippocampus. Neuron 33, 325–340.
Castle, M., Comoli, E., Loewy, A.D., 2005. Autonomic brainstem nuclei are linked to the hippocampus. Neuroscience 134, 657–669.
Chauviere, L., Rafrafi, N., Thinus-Blanc, C., Bartolomei, F., Esclapez, M., Bernard, C., 2009. Early deficits in spatial memory and theta rhythm in experimental temporal lobe epilepsy. J. Neurosci. 29, 5402–5410.
Cimpianu, C.L., Strube, W., Falkai, P., Palm, U., Hasan, A., 2017. Vagus nerve stimulation in psychiatry: a systematic review of the available evidence. J. Neural. Transm. (Vienna) 124, 145–158.
Colom, L.V., 2006. Septal networks: relevance to theta rhythm, epilepsy and Alzheimer's disease. J. Neurochem. 96, 609–623.
Díaz-Güemes Martín-Portugués, I., Sánchez Margallo, F.M., Pascual Sánchez-Gijón, S., Crisóstomo Ayala, V., Usón Gargallo, J., 2005. Histopathologic features of the vagus nerve after electrical stimulation in swine. Histol. Histopathol. 20, 851–856.
Dahlin, L.B., Rydevik, B., McLean, W.G., Sjöstrand, J., 1984. Changes in fast axonal transport during experimental nerve compression at low pressures. Exp. Neurol. 84, 29–36.
De Ferrari, G.M., Schwartz, P.J., 2011. Vagus nerve stimulation: from pre-clinical to clinical application: challenges and future directions. Heart Fail. Rev. 16, 195–203.
Dorr, A.E., Debonnel, G., 2006. Effect of vagus nerve stimulation on serotonergic and noradrenergic transmission. J. Pharmacol. Exp. Ther. 318, 890–898.
Geddes, L.A., Roeder, R., 2003. Criteria for the selection of materials for implanted electrodes. Ann. Biomed. Eng. 31, 879–890.
Hays, S.A., Ruiz, A., Bethea, T., Khodaparast, N., Carmel, J.B., Rennaker 2nd, R.L., Kilgard, M.P., 2016. Vagus nerve stimulation during rehabilitative training enhances recovery of forelimb function after ischemic stroke in aged rats. Neurobiol. Aging 43, 111–118.
Howland, R.H., Shutt, L.S., Berman, S.R., Spotts, C.R., Denko, T., 2011. The emerging use of technology for the treatment of depression and other neuropsychiatric disorders. Ann. Clin. Psychiatry 23, 48–62.
Howland, R.H., 2014. Vagus nerve stimulation. Curr. Behav. Neurosci. Rep. 1, 64–73.
Huerta, P.T., Lisman, J.E., 1995. Bidirectional synaptic plasticity induced by a single burst during cholinergic theta oscillation in CA1 in vitro. Neuron 15, 1053–1063.
Hyman, B.T., Van Hoesen, G.W., Damasio, A.R., Barnes, C.L., 1984. Alzheimer's disease: cell-specific pathology isolates the hippocampal formation. Science 225, 1168–1170.
Kang, D., Ding, M., Topchiy, I., Shifflett, L., Kocsis, B., 2015. Theta-rhythmic drive between medial septum and hippocampus in slow-wave sleep and microarousal: a Granger causality analysis. J. Neurophysiol. 114, 2797–2803.
Kramis, R., Vanderwolf, C.H., Bland, B.H., 1975. Two types of hippocampal rhythmical slow activity in both the rabbit and the rat: relations to behavior and effects of atropine diethyl ether, urethane, and pentobarbital. Exp. Neurol. 49, 58–85.
Lanska, D.J., 2002. J.L. Corning and vagal nerve stimulation for seizures in the 1880. Neurology 58, 452–459.
Larsen, L.E., Wadman, W.J., Marinazzo, D., van Mierlo, P., Delbeke, J., Daelemans, S., Sprengers, M., Thyrion, L., et al., 2016a. Vagus nerve stimulation applied with a rapid cycle has more profound influence on hippocampal electrophysiology than a standard cycle. Neurotherapeutics 13, 592–602.
Larsen, L.E., Wadman, W.J., van Mierlo, P., Delbeke, J., Grimonprez, A., Van Nieuwenhuyse, B., Portelli, J., Boon, P., et al., 2016b. Modulation of hippocampal activity by vagus nerve stimulation in freely moving rats. Brain Stimul. 9, 124–132.
Lee, M.G., Chrobak, J.J., Sik, A., Wiley, R.G., Buzsáki, G., 1994. Hippocampal theta activity following selective lesion of the septal cholinergic systems. Neuroscience 2, 1033–1047.
Mauskop, A., 2005. Vagus nerve stimulation relieves chronic refractory migraine and cluster headaches. Cephalalgia 25, 82–86.
McCreery, D.B., Agnew, W.F., Yuen, T.G., Bullara, L.A., 1992. Damage in peripheral nerve from continuous electrical stimulation: comparison of two stimulus waveforms. Med. Biol. Eng. Comput. 30, 109–114.
Mehta, M.R., 2015. From synaptic plasticity to spatial maps and sequence learning. Hippocampus 25, 756–762.
Merrill, C.A., Jonsson, M.A., Minthon, L., Ejnell, H., C-son Silander, H., Blennow, K., Karlsson, M., Nordlund, A., et al., 2006. Vagus nerve stimulation in patients with Alzheimer's disease: additional follow-up results of a pilot study through 1 year. J. Clin. Psychiatry 67, 1171–1178.
Mesbah-Oskui, L., Georgiou, J., Roder, J.C., 2015. Hippocampal place cell and inhibitory neuron activity in Disrupted-in-schizophrenia-1 mutant mice: implications for working memory deficits. NPJ Schizophr. 1, 15011.
Monmaur, P., Breton, P., 1991. Elicitation of hippocampal theta by intraseptal carbachol injection in freely moving rats. Brain Res. 544, 150–155.
Natsume, K., Kometani, K., 1997. Theta-activity-dependent and −independent muscarinic facilitation of long-term potentiation in guinea pig hippocampal slices. Neurosci. Res. 27, 335–341.
Neren, D., Johnson, M.D., Legon, W., Bachour, S.P., Ling, G., Divani, A.A., 2016. Vagus nerve stimulation and other neuromodulation methods for treatment of traumatic brain injury. Neurocrit. Care 24, 308–319.
Ochoa, J., Fowler, T.J., Gilliatt, R.W., 1972. Anatomical changes in peripheral nerves compressed by a pneumatic tourniquet. J. Anat. 113, 433–455.
Oddie, S.D., Bland, B.H., 1998. Hippocampal formation theta activity and movement selection. Neurosci. Biobehav. Rev. 22, 221–231.
Oddie, S.D., Bland, B.H., Colom, L.V., Vertes, R.P., 1994. The midline posterior hypothalamic region comprises a critical part of the ascending brainstem hippocampal synchronizing pathway. Hippocampus 4, 454–473.

Ordonez, J.S., Pikov, V., Wiggins, H., Patten, C., Stieglitz, T., Rickert, J., Schuettler, M., 2014. Cuff electrodes for very small diameter nerves – prototyping and first recordings in vivo. Conf. Proc. IEEE Eng. Med. Biol. Soc. 2014, 6846–6849.
Paxinos, G., Watson, C., 2014. The Rat Brain in Stereotaxic Coordinates, 7th ed. Academic Press, San Diego.
Picq, C.A., Clarençon, D., Sinniger, V.E., Bonaz, B.L., Mayol, J.F., 2013. Impact of anesthetics on immune functions in a rat model of vagus nerve stimulation. PLoS One 8, e67086.
Pu, Y., Cornwell, B.R., Cheyne, D., Johnson, B.W., 2017. The functional role of human right hippocampal/parahippocampal theta rhythm in environmental encoding during virtual spatial navigation. Hum. Brain Mapp. 38, 1347–1361.
Rodríguez, F.J., Ceballos, D., Schüttler, M., Valero, A., Valderrama, E., Stieglitz, T., Navarro, X., 2000. Polyimide cuff electrodes for peripheral nerve stimulation. J. Neurosci. Methods 98, 105–118.
Rose, T.L., Robblee, L.S., 1990. Electrical stimulation with Pt electrodes. VIII. Electrochemically safe charge injection limits with 0.2 ms pulses. EEE Trans. Biomed. Eng. 37, 1118–1120.
Sainsbury, R.S., Partlo, L.A., 1993. Alpha 2 modulation of type 1 and type 2 hippocampal theta in the freely moving rat. Brain Res. Bull. 31, 437–442.
Sainsbury, S., 1985. Type 2 theta in the guinea pig and the cat. In: Buzsáki, G., Vanderwolf, C.H. (Eds.), Electrical Activity of the Archicortex. Akademiai Kiado, Budapest, pp. 11–22.
Slot, P.J., Selmar, P., Rasmussen, A., Sinkjaer, T., 1997. Effect of long-term implanted nerve cuff electrodes on the electrophysiological properties of human sensory nerves. Artif. Organs 21, 207–209.
Stevenson, M., Baylor, K., Netherton, B.L., Stecker, M.M., 2010. Electrical stimulation and electrode properties. Part 2: pure metal electrodes. Am. J. Electroneurodiagnostic Technol. 50, 263–296.
Van Bockstaele, E.J., Peoples, J., Telegan, P., 1999. Efferent projections of the nucleus of the solitary tract to peri-locus coeruleus dendrites in rat brain: evidence for a monosynaptic pathway. J. Comp. Neurol. 412, 410–428.
Vanderwolf, C.H., 1969. Hippocampal electrical activity and voluntary movement in the rat. Electroencephalogr. Clin. Neurophysiol. 26, 407–418.
Vanhoestenberghe, A., 2013. Chronic nerve root entrapment: compression and degeneration. J. Neural. Eng. 10, 011001.
Vertes, R.P., Kocsis, B., 1997. Brainstem-diencephalo-septohippocampal systems controlling the theta rhythm of the hippocampus. Neuroscience 8, 893–926.
Woodbury, D.M., Woodbury, J.W., 1990. Effects of vagal stimulation on experimentally induced seizures in rats. Epilepsia 31, S7–19.
Xiang, Y.X., Wang, W.X., Xue, Z., Zhu, L., Wang, S.B., Sun, Z.H., 2015. Electrical stimulation of the vagus nerve protects against cerebral ischemic injury through an anti-infammatory mechanism. Neural Regen. Res. 10, 576–582.
Yuen, T.G., Agnew, W.F., Bullara, L.A., 1984. Histopathological evaluation of dog sacral nerve after chronic electrical stimulation for micturition. Neurosurgery 14, 449–455.